J. Fluid Mech. (1998), *vol.* 357, *pp.* 249–278. Printed in the United Kingdom

© 1998 Cambridge University Press

Inertial and viscous effects on dynamic contact angles

By R. G. COX†

Department of Civil Engineering and Applied Mechanics, McGill University, Montreal, Quebec, Canada

(Received 15 November 1996 and in revised form 10 October 1997)

An investigation is made into the dynamics involved in the movement of the contact line when a single liquid with an interface moves into a vacuum over a smooth solid surface. In order to remove the stress singularity at the contact line, it is postulated that slip between the liquid and the solid or some other mechanism occurs very close to the contact line. It is assumed that the flow produced is inertia dominated with the Reynolds number based on the slip length being very large. Following a procedure similar to that used by Cox (1986) for the viscous-dominated situation (in which the Reynolds number based on the macroscopic length scale was assumed very small) using matched asymptotic expansions, we obtain the dependence of the macroscopic dynamic contact angle on the contact line velocity over the solid surface for small capillary number and small slip length to macroscopic lengthscale ratio. These results for the inertia-dominated situation are then extended (at the lowest order in capillary number) to an intermediate Reynolds number situation with the Reynolds number based on the slip length being very small and that based on the macroscopic lengthscale being very large.

1. Introduction

Consider a liquid in contact with a smooth solid surface with an interface which intersects the solid surface at a contact line. If this contact line is constrained to move across the solid surface with a speed U, it is known that the contact angle (i.e. the angle between the interface and the solid surface at the contact line measured through the liquid) increases or decreases as the magnitude of U increases according to whether the liquid is advancing or receding (Dussan V. 1979). We consider here the dynamics of such contact line movement and assume that on the side of the interface away from the liquid there is a vacuum (or at least a fluid, such as the liquid vapour, of sufficiently low viscosity and density that it plays no significant role in the dynamics). It is the object of the present paper to predict how the contact angle will vary with the contact line velocity U under such a situation by calculating the liquid interface shape near the contact line due to the action of the stresses in the liquid produced by the motion. Examples of contact line movement across a solid surface occur with (*a*) the spreading of a liquid drop on a horizontal surface (Greenspan 1978; Hocking & Rivers 1982), (*b*) the movement of a drop down an inclined surface, (*c*) the movement of a meniscus along a tube, (*d*) the movement of a solid object

† Professor Cox died before this paper was completed. This manuscript was prepared for submission and publication, with some additional footnotes, by J. R. A. Pearson, 23 Chaucer Road, Cambridge CB2 2EB, UK.

https://doi.org/10.1017/S0022112097008112 Published online by Cambridge University Press

such as a plate or a sphere through a liquid interface and (*e*) in printing, coating and painting processes.

When the flow field is calculated in the neighbourhood of a moving contact line it is found that for all contact angles other than 180° there is a non-integrable singularity in the stress at the contact line resulting in a divergent integral for the drag force on the solid boundary. In order to avoid this problem slip has been postulated to occur between the liquid and solid surface at small distances of order s say, from the contact line (Dussan V. 1976; Hocking 1977; Huh & Mason 1977*b*; Hocking & Rivers 1982; Cox 1986). The following models for this slip have been used:

(i) Zero tangential stress at the solid surface at distances from the contact line less than s and no slip for distances greater than s (Huh & Mason 1977*b*).

(ii) The difference in tangential velocity between liquid and solid (slip velocity) is proportional to the local shear velocity gradient at the solid surface (Hocking 1977; Huh & Mason 1977*b*; Lowndes 1980).

(iii) The slip velocity is algebraically dependent upon distance from the contact line (Dussan V. 1976).

The slip models (i) and (ii) are considered in the present paper together with a more general form of the slip model (ii), namely

(iv) The difference in tangential velocity between liquid and solid is proportional to the local shear velocity gradient raised to the power of p (where $p > 0$).

Slip between liquid and solid is a convenient assumption to make in order to get rid of the non-integrable stress singularity, but there are also other possibilities for the removal of the singularity by taking into account non-continuum effects†, non-Newtonian fluid effects and the elasticity of the solid. Hocking & Rivers (1982) considered the spreading of a drop of very viscous liquid on a smooth horizontal surface using singular perturbation expansion methods. This theory was then extended to more general spreading situations by Cox (1986) who considered contact line movement for a general geometry in which one fluid displaces a second fluid with which the first is immiscible for the special situation in which the flow everywhere is viscous dominated (and therefore satisfies the Stokes equations), which occurs if the Reynolds number based on the macroscopic (experimental) lengthscale R is very much smaller than unity. The flow field and the interface shape were found by making a singular perturbation expansion in the capillary number $Ca \equiv \mu U/\sigma$ (where U is a characteristic velocity, μ the viscosity and σ the interfacial tension) and the ratio of slip length s to macroscopic lengthscale R, $\varepsilon = s/R$ where it was assumed that

$$Ca \ll 1, \quad \varepsilon \ll 1. \tag{1.1}$$

It was found that two regions of expansion were necessary if, as $Ca \to 0$, $\varepsilon \to 0$, we let $(Ca \ln \varepsilon^{-1}) \to 0$, in which case the interface was almost planar, but that three regions of expansion were necessary if, as $Ca \to 0$, $\varepsilon \to 0$, the quantity $(Ca \ln \varepsilon^{-1})$ was fixed and of order unity. In this latter situation, the slope angle that the interface makes with the solid surface can change by an amount of order unity. A macroscopic contact

† If molecular effects are to be taken into account, then steep gradients in fluid density arise in the neighbourhood of interfaces and contact lines; in the case of moving contact lines, these interfaces will not be at equilibrium in a thermodynamic sense. The width of these regions of rapid change will be of the order of a few (3–10) molecules, though the distance from the contact line at which significant disequilibrium arises may be much larger. The slip models (i)–(iv) above can be regarded as coarse approximations relevant on length scales larger than a few nanometres; it is worth noting that the standard concepts of interfacial and surface tension are analogous approximations for equilibrium systems away from contact lines.

https://doi.org/10.1017/S0022112097008112 Published online by Cambridge University Press

angle was defined in terms of the asymptotic form of the macroscopic (experimental) lengthscale of the slope angle that the interface makes with the solid surface as the contact line is approached. Then from the form of the interface shape very close to the contact line, an expression for the macroscopic contact angle was obtained in terms of the contact line speed U and the microscopic contact angle defined as the angle the liquid interface makes with the solid surface at distances from the contact line of order of the slip lengthscale† s. This theory gives results which agree very well with the experiments of Hoffman (1975) and of Hocking & Rivers (1982) if it is assumed that the microscopic contact angle is a constant independent of the spreading velocity U and possesses a value which depends only on the particular liquid and solid surface being considered‡.

This theory of Cox (1986) for one fluid displacing a second immiscible fluid may be used in the special case we are considering in the present paper with just a single liquid (by letting the viscosity of the second fluid tend to zero) so long as the Reynolds number based on the macroscopic lengthscale R is very much smaller than unity.

In the present paper we obtain first the relationship between the macroscopic contact angle and contact line velocity for the situation of a single advancing liquid (§§ 2–7) when the flow so produced is inertia dominated everywhere requiring that the Reynolds number based on the slip length s be very large compared with unity. This is done for the situation in which the conditions (1.1) are satisfied.

Then in §§ 8 and 9 the theory is extended to an advancing liquid for which the situation is intermediate between the viscous situation (examined by Cox 1986) and the inertial situation (examined in §§ 2–7) with again the conditions (1.1) being satisfied. Thus results expressing the macroscopic contact angle in terms of contact line velocity are obtained for an advancing liquid which covers the complete range of Reynolds number (so long as (1.1) is satisfied).

2. General problem

For the spreading of a Newtonian liquid of viscosity μ and density ρ on a solid surface, it will be assumed that the slip length s is much smaller than a characteristic macroscopic lengthscale R so that

$$\varepsilon \equiv \frac{s}{R} \ll 1 \tag{2.1}$$

and also that the capillary number Ca is small so that

$$Ca \equiv \mu \frac{U}{\sigma} \ll 1, \tag{2.2}$$

where U is a characteristic velocity of the spreading process and σ the surface tension of the liquid. This spreading liquid is assumed to move into a vacuum or to displace an immiscible fluid of very small density and viscosity (so that the role of this second fluid is negligible in the spreading process). The macroscopic Reynolds number Re of

† Clearly the notion of contact angle implies that the 'continuum approximation' involving infinitely thin interfaces and smooth surfaces can be made. The distinction made above between macroscopic and microscopic contact angles hence requires a large ratio in length between (each pair of) the interface thickness, the slip length s and the flow scale R; it also implies that gradients in the slope angle near the contact line are small enough for contact angles to be defined.

‡ This independence of U is a crucial one; it does not necessarily follow from thermodynamic arguments (Shikhmurzaev 1997).

https://doi.org/10.1017/S0022112097008112 Published online by Cambridge University Press

the flow produced, defined as

$$Re \equiv \frac{UR}{\nu}, \tag{2.3}$$

where $\nu = \mu/\rho$ and ρ is a constant density, is taken to be much larger than ε^{-1} (i.e. $Re \gg \varepsilon^{-1} \gg 1$) implying that we have an inertia-dominated flow (except in boundary layers) even at the slip lengthscale s since then

$$\varepsilon Re \equiv \frac{Us}{\nu} \gg 1. \tag{2.4}$$

Furthermore, for simplicity, we shall consider only situations in which (*a*) the spreading liquid is advancing (not receding) over the solid surface, (*b*) the contact line is moving normal to its direction over the surface, (*c*) the solid surface is smooth and essentially planar on lengthscales small compared with s (although it could possess a curvature of order R^{-1}). Also relative to suitably chosen coordinates (moving with the contact line) we assume (*d*) the liquid motion is steady and (*e*) the solid surfaces present, as well as the liquid interface, have zero normal velocity and hence only possess tangential motion. This means that in the limit of $\varepsilon Re \to \infty$, the liquid would be at rest apart from flow within boundary layers on the solid surfaces†. However at large but finite values of εRe, because of the flux of fluid into such boundary layers, an inviscid‡ flow would be induced in the liquid exterior to these boundary layers. Thus one might consider, for example, a thin flat solid plate moving steadily in its own plane through a liquid interface into the liquid or the steady motion of a liquid meniscus advancing along a uniform tube. Further assumptions to be made are that, in the region of interest near a contact line, (*f*) there is no boundary layer separation, (*g*) the boundary layer is laminar and (*h*) there is no inviscid flow (irrotational or rotational) induced resulting from motion outside the region of interest (at distances of order R from the contact line).

Whilst in §§ 3–6 the shape of the liquid interface is determined correct to order Ca^{+1} for situations where the above assumptions apply, a discussion is given in § 7 of the effect of removing assumptions (*a*), (*b*) and (*h*). Then in § 8, the effect of the replacement of condition (2.4) by

$$\varepsilon Re \ll 1, \quad Re \gg 1 \tag{2.5}$$

(or $1 \ll Re \ll \varepsilon^{-1}$) is considered so that the flow is viscous dominated at the slip lengthscale s but inertia dominated at the macroscopic lengthscale R. The results for this situation, intermediate between the viscous-dominated flow of Cox (1986) and the inertia-dominated flow, are then discussed in § 9.

3. Outer region

If the dimensional fluid velocity and pressure are $\boldsymbol{u}$ and p respectively at position $\boldsymbol{r}$, we define an outer region of expansion valid everywhere except close to the contact

† This restriction should perhaps be regarded as part of assumption (*h*); it is true that in the limit $\varepsilon Re \to \infty$, the motion of the plate will not induce any flow, but it needs to be proved that the only steady external flow is a rest state; even if this is the case, there is the issue of relating the results that flow from this assumption to realistic flow fields involving moving interfaces.

‡ Perhaps this is better stated as 'largely inviscid', as implied by (3.3). As will be seen later, it is the outer vorticity which is the key issue for the outer flow; an (irrotational) planar sink flow into the contact line need not necessarily be ruled out at this point.

https://doi.org/10.1017/S0022112097008112 Published online by Cambridge University Press

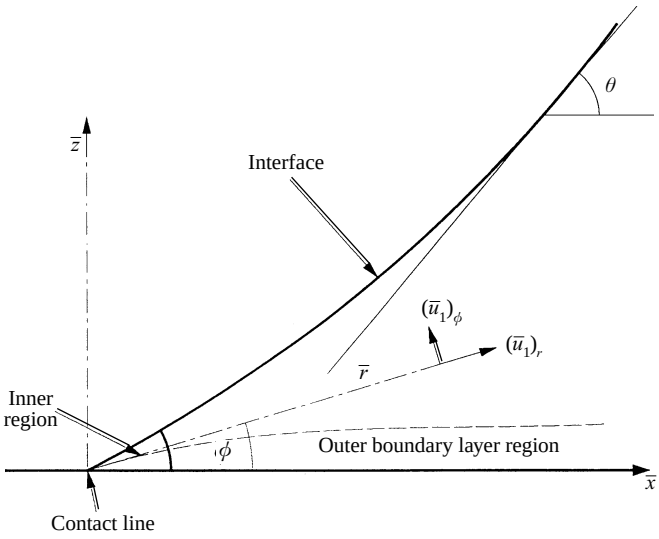


FIGURE 1. The outer flow region, showing Cartesian and polar coordinates.

line using (overbarred) outer variables made dimensionless by R, U and ρ. Thus

$$\bar{\boldsymbol{r}} = \boldsymbol{r}/R, \quad \bar{\boldsymbol{u}} = \boldsymbol{u}/U, \quad \bar{p} = p/(\rho U^2), \tag{3.1}$$

so that in this outer region

$$\left.\begin{aligned} Re^{-1}(\bar{\nabla}^2\bar{\boldsymbol{u}}) \; - \bar{\nabla}\bar{p} \; &= \bar{\boldsymbol{u}}\cdot\bar{\nabla}\bar{\boldsymbol{u}}, \\ \bar{\nabla}\cdot\bar{\boldsymbol{u}} &= 0. \end{aligned}\right\} \tag{3.2}$$

As mentioned in § 2, this outer region must be subdivided into a boundary layer region (or regions) valid near solid boundaries and an 'inviscid' flow region valid elsewhere where (3.2) is valid as written. Then if we expand the flow field $\bar{\boldsymbol{u}}$, $\bar{p}$ for small Re^{-1} in the inviscid region as

$$\bar{\boldsymbol{u}} = \bar{\boldsymbol{u}}_0 + \ldots, \quad \bar{p} = \bar{p}_0 + \ldots, \tag{3.3}$$

we see from (3.2) that $\bar{\boldsymbol{u}}_0$, $\bar{p}_0$ satisfy the inviscid Euler equations

$$-\bar{\nabla}\bar{p}_0 = \bar{\boldsymbol{u}}_0\cdot\bar{\nabla}\bar{\boldsymbol{u}}_0, \quad \bar{\nabla}\cdot\bar{\boldsymbol{u}}_0 = 0. \tag{3.4}$$

Then by assumption (*h*) in § 2, we see that $\bar{\boldsymbol{u}}_0$ is irrotational and must furthermore be a zero flow by the assumption (*e*) in § 2, i.e.

$$\bar{\boldsymbol{u}}_0 = 0, \quad \bar{p}_0 = \text{constant } (= P_0 \text{ say}). \tag{3.5}$$

Since, for matching purposes near the contact line, we shall later require only the lowest-order asymptotic form of the flow and interface shape in this outer expansion as we approach the contact line, we may take the solid surface locally near any given point P on the contact line to be planar with the contact line being straight and perpendicular to the direction of the solid surface motion (see assumption (*e*) in § 2). Thus if we take local outer-region Cartesian coordinates $(\bar{x}, \bar{y}, \bar{z})$ with origin at the point P on the contact line with the $\bar{z}$-axis normal to the planar surface and the $\bar{x}$-axis in the direction of the solid surface motion (relative to the interface), so that the $\bar{y}$-axis is directed along the contact line (see figure 1), then, by the assumption (*b*) in § 2, the fluid velocity is two-dimensional with $\bar{\boldsymbol{u}} = (\bar{u}, 0, \bar{w})$ where $\bar{u}, \bar{w}$ and $\bar{p}$ are

https://doi.org/10.1017/S0022112097008112 Published online by Cambridge University Press

functions only of $\bar{x}$ and $\bar{z}$. Boundary layer (double overbarred) variables to be used in the boundary layer region are then defined as

$$\left.\begin{array}{llll} \bar{\bar{x}} = \bar{x}, & \bar{\bar{y}} = \bar{y}, & \bar{\bar{z}} = Re^{1/2}\bar{z}, & \\ \bar{\bar{u}} = \bar{u}, & \bar{\bar{v}} = \bar{v}, & \bar{\bar{w}} = Re^{1/2}\bar{w}, & \bar{\bar{p}} = \bar{p}, \end{array}\right\} \tag{3.6}$$

so that in these variables (with $\bar{\bar{v}} = \bar{v} = 0$) the equations (3.2) become

$$\left.\begin{array}{c} Re^{-1}\dfrac{\partial^2\bar{\bar{u}}}{\partial\bar{\bar{x}}^2} + \dfrac{\partial^2\bar{\bar{u}}}{\partial\bar{\bar{z}}^2} - \dfrac{\partial\bar{\bar{p}}}{\partial\bar{\bar{x}}} = \bar{\bar{u}}\dfrac{\partial\bar{\bar{u}}}{\partial\bar{\bar{x}}} + \bar{\bar{w}}\dfrac{\partial\bar{\bar{u}}}{\partial\bar{\bar{z}}}, \\ Re^{-2}\dfrac{\partial^2\bar{\bar{w}}}{\partial\bar{\bar{x}}^2} + Re^{-1}\dfrac{\partial^2\bar{\bar{w}}}{\partial\bar{\bar{z}}^2} - \dfrac{\partial\bar{\bar{p}}}{\partial\bar{\bar{z}}} = Re^{-1}\left(\bar{\bar{u}}\dfrac{\partial\bar{\bar{w}}}{\partial\bar{\bar{x}}} + \bar{\bar{w}}\,\dfrac{\partial\bar{\bar{w}}}{\partial\bar{\bar{z}}}\right), \\ \dfrac{\partial\bar{\bar{u}}}{\partial\bar{\bar{x}}} + \dfrac{\partial\bar{\bar{w}}}{\partial\bar{\bar{z}}} = 0. \end{array}\right\} \tag{3.7}$$

Then by expanding $\bar{\bar{u}}$, $\bar{\bar{w}}$ and $\bar{\bar{p}}$ for small Re^{-1} as

$$\bar{\bar{u}} = \bar{\bar{u}}_0 + \ldots, \quad \bar{\bar{w}} = \bar{\bar{w}}_0 + \ldots, \quad \bar{\bar{p}} = \bar{\bar{p}}_0 + \ldots, \tag{3.8}$$

we see by substituting into (3.7) and by matching onto the known form of the inviscid flow solution (3.3) and (3.5) that $\bar{\bar{u}}_0$ and $\bar{\bar{w}}_0$ satisfy the boundary layer equations

$$\frac{\partial^2\bar{\bar{u}}_0}{\partial\bar{\bar{z}}^2} = \bar{\bar{u}}_0\frac{\partial\bar{\bar{u}}_0}{\partial\bar{\bar{x}}} + \bar{\bar{w}}_0\frac{\partial\bar{\bar{u}}_0}{\partial\bar{\bar{z}}}, \quad \frac{\partial\bar{\bar{u}}_0}{\partial\bar{\bar{x}}} + \frac{\partial\bar{\bar{w}}_0}{\partial\bar{\bar{z}}} = 0, \tag{3.9}$$

with $\bar{\bar{p}}_0 = P_0$ everywhere. Also matching requires that

$$\bar{\bar{u}}_0 \to 0 \quad \text{as} \quad \bar{\bar{z}} \to \infty. \tag{3.10}$$

On the solid surface ($\bar{\bar{z}} = 0$), if we take the characteristic velocity U to be the spreading velocity at the chosen point P, we see that the no-slip boundary condition is

$$\bar{\bar{u}}_0 = +1, \quad \bar{\bar{w}}_0 = 0 \quad \text{on} \quad \bar{\bar{z}} = 0 \quad (\bar{\bar{x}} \geqslant 0). \tag{3.11}$$

Such a steady boundary layer for $\bar{\bar{x}} \geqslant 0$, which starts at $\bar{\bar{x}} = 0$ for which we have unit velocity at the wall and zero velocity parallel to the wall at large distances from the wall, was studied by Sakiadis (1961) who showed that there must be a fluid inflow into the boundary layer with

$$\bar{\bar{w}}_0 \sim -\tfrac{1}{2}\alpha^*\,\bar{\bar{x}}^{-1/2} \quad \text{as} \quad \bar{\bar{z}} \to \infty \tag{3.12}$$

where

$$\alpha^* = 1.616\,05. \tag{3.13}$$

By matching this onto the inviscid solution $\bar{\boldsymbol{u}}, \bar{p}$ we see from (3.6) that

$$\bar{w} \sim -\tfrac{1}{2}\alpha^*\bar{x}^{-1/2}Re^{-1/2} \quad \text{as} \quad \bar{z} \to 0, \tag{3.14}$$

so that the inviscid velocity $\bar{\boldsymbol{u}}$ is of order $Re^{-1/2}$ and the inviscid pressure $\bar{p}$, by (3.2), of order Re^{-1}. Thus we write, for $Re^{-1} \to 0$,

$$\bar{\boldsymbol{u}} = Re^{-1/2}\,\bar{\boldsymbol{u}}_1 + \ldots, \quad \bar{p} = Re^{-1}\,\bar{p}_1 + \ldots, \tag{3.15}$$

which, when substituted into (3.2), gives at order Re^{-1} the Euler equations

$$-\bar{\nabla}\bar{p}_1 = \bar{\boldsymbol{u}}_1 \cdot \bar{\nabla}\bar{\boldsymbol{u}}_1, \quad \nabla \cdot \bar{\boldsymbol{u}}_1 = 0. \tag{3.16}$$

https://doi.org/10.1017/S0022112097008112 Published online by Cambridge University Press

It therefore follows from assumption (*h*) in § 2 that $\bar{\boldsymbol{u}}_1$ is irrotational so that

$$\nabla \times \bar{\boldsymbol{u}}_1 = 0, \quad \nabla \cdot \bar{\boldsymbol{u}}_1 = 0, \tag{3.17}$$

with $\bar{p}_1$ being determined by Bernoulli's equation which may be written as

$$\bar{p} + \tfrac{1}{2}|\bar{\boldsymbol{u}}|^2 = \Delta\overline{P}$$

or as

$$\bar{p}_1 + \tfrac{1}{2}|\bar{\boldsymbol{u}}_1|^2 = Re\Delta\overline{P} \tag{3.18}$$

where $\Delta\overline{P}$ is a constant (or a hydrostatic pressure variation if gravity effects are significant).

If $\bar{n}$ is normal distance (in the $\bar{\boldsymbol{r}}$-variables) from the liquid interface measured positively into the liquid then the dimensional normal stress that the liquid exerts on the interface is

$$-\rho U^2\bar{p} + 2\mu\frac{U}{R}\frac{\partial\bar{u}}{\partial\bar{n}} = \rho U^2\left[-\bar{p} + 2Re^{-1}\frac{\partial\bar{u}}{\partial\bar{x}}\right] = \rho U^2\left[-Re^{-1}\bar{p}_1 + O(Re^{-3/2})\right].$$

The normal stress boundary condition at the liquid interface that this normal stress be equal to σ times the interface curvature, may be written as

$$\frac{\sigma\bar{\kappa}}{R} = \rho U^2(-Re^{-1}\bar{p}_1) = \rho U^2(-\Delta\overline{P} + \tfrac{1}{2}Re^{-1}|\bar{\boldsymbol{u}}_1|^2), \tag{3.19}$$

where $\bar{\kappa} = R\kappa$ is the dimensionless interface curvature (with κ being interface curvature defined as positive for centre of curvature on the side away from the liquid). This boundary condition (3.19) may be written in the form

$$\bar{\kappa} = -Ca\ \bar{p}_1 = -\Delta\overline{P}^* + \tfrac{1}{2}Ca|\bar{\boldsymbol{u}}_1|^2 \tag{3.20}$$

where Ca is the capillary number defined by (2.2) and where

$$\Delta\overline{P}^* = \frac{\rho U^2 R}{\sigma}\Delta\overline{P} \tag{3.21}$$

is the pressure drop across the interface (made dimensionless by the pressure σ/R) which would occur in the absence of fluid motion. If the Bond number $B \equiv \rho g R^2/\sigma$ is very small, $\Delta\overline{P}^*$ may be taken as constant, whereas otherwise a hydrostatic pressure variation should be included in $\Delta\overline{P}^*$. However even in this latter case, the effects of hydrostatic pressure variation are negligible on the asymptotic solution which we are considering here of approaching the contact line in this outer region.

In addition to the normal stress boundary condition (3.20) on the liquid interface we also require zero normal velocity so that

$$\boldsymbol{n} \cdot \bar{\boldsymbol{u}}_1 = 0 \tag{3.22}$$

on the liquid interface (where $\boldsymbol{n}$ is a unit normal vector to that interface).

Since $\bar{\boldsymbol{u}}_1, \bar{p}_1$ is two-dimensional (like $\bar{\boldsymbol{u}}, \bar{p}$), we write $\bar{\boldsymbol{u}}_1 = (\bar{u}_1, 0, \bar{w}_1)$ where $\bar{u}_1, \bar{w}_1$ and $\bar{p}_1$ are functions only of $\bar{x}$ and $\bar{z}$. Then, from (3.14), we see that

$$\bar{w}_1 = -\tfrac{1}{2}\alpha^*\bar{x}^{-1/2} \quad \text{on} \quad \bar{z} = 0. \tag{3.23}$$

Thus the inviscid flow velocity $\bar{\boldsymbol{u}}_1$ satisfies (3.17) with the boundary conditions (3.20) and (3.22) on the liquid interface and (3.23) on the solid surface. In order to solve for $\bar{\boldsymbol{u}}_1$ and the interface shape in the outer region (as the contact line is approached), we set up a plane polar coordinate system $(\bar{r}, \phi)$ in the $(\bar{x}, \bar{z})$-plane of the outer inviscid

https://doi.org/10.1017/S0022112097008112 Published online by Cambridge University Press

region with origin at P with $\phi = 0$ in the solid surface directed in the $\bar{x}$-direction (see figure 1).

Considering the flow $\bar{\boldsymbol{u}}_1, \bar{p}_1$ and the interface shape as an expansion in the small capillary number Ca (see (2.2)) we see that at order Ca^0, the interface shape is, from (3.20), given by

$$\bar{\kappa} = -\Delta \bar{P}^*$$

which, for $\bar{x} \to 0$ has the solution

$$\bar{z} = (\tan \theta'_m)\bar{x} + O(\bar{x}^2)$$

or, in terms of the polar coordinates, for $\bar{r} \to 0$ as

$$\phi = \theta'_m + O(\bar{r}), \tag{3.24}$$

where θ'_m is a constant. If we define θ as the angle the tangent to the interface makes with the solid surface at a general position on the interface (see figure 1) so that

$$\theta = \left[\phi + \tan^{-1}\left(\bar{r}\frac{\mathrm{d}\phi}{\mathrm{d}\bar{r}}\right)\right]\Bigg|_{\text{interface}} \tag{3.25}$$

then we see from (3.24) that at order Ca^0, the interface may also be written as

$$\theta = \theta'_m + O(\bar{r}) \tag{3.26}$$

for $\bar{r} \to 0$†.

The flow field $\bar{\boldsymbol{u}}_1, \bar{p}_1$ at order Ca^0 is thus the solution of (3.17) with (3.22) applied on the surface (3.24) (i.e. the liquid interface at order Ca^0) and with (3.23) applied on the solid surface $\phi = 0$. Then if $\bar{\psi}_1$ is the stream function corresponding to the velocity field $\bar{\boldsymbol{u}}_1$ at order Ca^0 so that its radial component $(\bar{u}_1)_r$ and transverse component $(\bar{u}_1)_\phi$ are

$$(\bar{u}_1)_r = \frac{1}{\bar{r}}\frac{\partial \bar{\psi}_1}{\partial \phi}, \quad (\bar{u}_1)_\phi = -\frac{\partial \bar{\psi}_1}{\partial \bar{r}}, \tag{3.27}$$

the above equations and boundary conditions for $\bar{\boldsymbol{u}}_1$ reduce to

$$\bar{\nabla}^2 \bar{\psi}_1 = 0 \tag{3.28}$$

with

$$\bar{\psi}_1 = \alpha^* \bar{r}^{1/2} \quad \text{on} \quad \phi = 0, \tag{3.29}$$

$$\bar{\psi}_1 = 0 \quad \text{on} \quad \phi = \theta'_m. \tag{3.30}$$

This possesses the solution

$$\bar{\psi}_1 = \alpha^* \bar{r}^{1/2}(\cos \tfrac{1}{2}\phi - \cot \tfrac{1}{2}\theta'_m \sin \tfrac{1}{2}\phi). \tag{3.31}$$

Thus

$$(\bar{u}_1)_r = -\tfrac{1}{2}\alpha^* \bar{r}^{-1/2}\left(\sin \tfrac{1}{2}\phi + \cot \tfrac{1}{2}\theta'_m \cos\ \tfrac{1}{2}\phi\right), \tag{3.32}$$

$$(\bar{u}_1)_\phi = -\tfrac{1}{2}\alpha^* \bar{r}^{-1/2}\left(\cos \tfrac{1}{2}\phi - \cot \tfrac{1}{2}\theta'_m \sin \tfrac{1}{2}\phi\right), \tag{3.33}$$

so that by (3.18) the corresponding pressure field $\bar{p}_1$ is

$$\bar{p}_1 = -\tfrac{1}{8}\alpha^{*2}\bar{r}^{-1}\mathrm{cosec}^2 \tfrac{1}{2}\theta'_m + \text{constant}. \tag{3.34}$$

† We should note that $|\bar{u}_1|^2$ is singular, $O(\bar{r}^{-1})$ as $\bar{r} \to O$, and so the term of $O(Ca)$ in (3.20) is also singular. θ'_m has therefore to be interpreted with that in mind. The consequences of this singularity become clearer later, in (3.37), where θ is shown to behave as $O(Ca \ln \bar{r})$.

https://doi.org/10.1017/S0022112097008112 Published online by Cambridge University Press

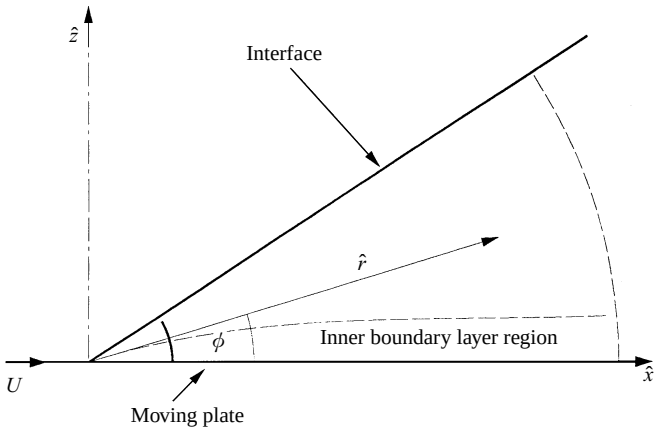


FIGURE 2. The inner flow region.

Hence from the form of the interface curvature given by (3.20), it is seen that the interface shape as $\bar{r} \to 0$ is

$$\theta \sim (\theta'_m + \ldots) + Ca\ \theta_1 + \ldots, \tag{3.35}$$

where

$$\frac{\mathrm{d}\theta_1}{\mathrm{d}\bar{r}} = \tfrac{1}{2}|\bar{\boldsymbol{u}}_1|^2 = \tfrac{1}{8}\alpha^{*2}\bar{r}^{-1}\mathrm{cosec}^2\tfrac{1}{2}\theta'_m\ . \tag{3.36}$$

(It should be noted that (3.35) and (3.36) assume a neglible Bond number.) Thus the liquid interface for $\bar{r} \to 0$ is

$$\theta \sim (\theta'_m + \ldots) + Ca\ (\tfrac{1}{8}\alpha^{*2}\mathrm{cosec}^2\tfrac{1}{2}\theta'_m \ln\bar{r} + Q_1 + \ldots) \tag{3.37}$$

where Q_1 is a constant of integration. Since the angle θ'_m is at present undetermined and since, as will be shown later, the value of θ'_m in any particular problem is itself a function of Ca (but is of order unity in the limit $Ca \to 0$) we may, for simplicity, absorb the term CaQ_1 into θ'_m by writing

$$\theta_m = \theta'_m + CaQ_1 \tag{3.38}$$

so that as $\bar{r} \to 0$, the liquid interface is

$$\theta \sim (\theta_m + \ldots) + Ca(\tfrac{1}{8}\alpha^{*2}\mathrm{cosec}^2\tfrac{1}{2}\theta_m \ln\bar{r} + \ldots). \tag{3.39}$$

The quantity θ_m, which we will refer to as the macroscopic constant angle, will be regarded as being determined by (3.39), the asymptotic form of the liquid interface shape as $\bar{r} \to 0$ in our outer region for any particular flow situation and spreading velocity.

4. Inner region

An inner region of expansion valid close to the contact line at P is defined in the same manner for the case where viscous forces dominate (Cox 1986) using variables made dimensionless by s, U and μ. We thus use Cartesian coordinates $(\hat{x}, \hat{z})$ or polar coordinates $(\hat{r}, \phi)$ (with origin at P moving with the contact line) as independent variables (see figure 2) where

$$\hat{x} = \varepsilon^{-1}\bar{x}, \quad \hat{z} = \varepsilon^{-1}\bar{z}, \quad \hat{r} = \varepsilon^{-1}\bar{r}. \tag{4.1}$$

https://doi.org/10.1017/S0022112097008112 Published online by Cambridge University Press

The velocity $\hat{\boldsymbol{u}}$ and pressure $\hat{p}$ are thus given in terms of the velocity $\bar{\boldsymbol{u}}$ and pressure $\bar{p}$ in the outer region by

$$\hat{\boldsymbol{u}} = \bar{\boldsymbol{u}} \quad \text{and} \quad \hat{p} = \bar{p}. \tag{4.2}$$

Since the Reynolds number (εRe) for flow in this inner region has been assumed (see (2.4)) to be large, the flow is inviscid apart from a boundary layer at the solid surface.

In the inner inviscid region outside the boundary layer the flow equations (3.2) become

$$\left.\begin{aligned}(\varepsilon Re)^{-1}(\hat{\nabla}^2\hat{\boldsymbol{u}}) - \hat{\nabla}\hat{p} = \hat{\boldsymbol{u}}\cdot\hat{\nabla}\hat{\boldsymbol{u}},\\ \hat{\nabla}\cdot\hat{\boldsymbol{u}} = 0,\end{aligned}\right\} \tag{4.3}$$

which at lowest order in the small parameter ($\varepsilon^{-1}Re^{-1}$) gives the inviscid Euler equations, which, as we have already seen, implies that $\hat{\boldsymbol{u}}$ is irrotational. In fact, as in the outer region, $\hat{\boldsymbol{u}}$ is zero at order $(\varepsilon^{-1}Re^{-1})^0$.

Within the inner boundary layer we use inner boundary layer coordinates $(\hat{\bar{x}}, \hat{\bar{z}})$, velocity $(\hat{\bar{u}}, \hat{\bar{w}})$ and pressure $\hat{\bar{p}}$ defined in a manner similar to the outer boundary layer variables (see (3.6)) but with Re replaced by εRe, i.e.

$$\hat{\bar{x}} = \hat{x}, \quad \hat{\bar{z}} = (\varepsilon Re)^{1/2}\hat{z}, \quad \hat{\bar{u}} = \hat{u}, \quad \hat{\bar{w}} = (\varepsilon Re)^{1/2}\hat{w}, \quad \hat{\bar{p}} = \hat{p}. \tag{4.4}$$

However, the slip length s, which is as yet undefined, must be chosen in a manner which is dependent on the slip law which applies at the solid surface. For example, let us consider the slip model considered by Hocking (1977), Huh & Mason (1977*b*) and Lowndes (1980) in which the difference in tangential velocity between liquid and solid is equal to a constant α multiplied by the shear velocity gradient at the solid surface $\hat{z} = 0$ so that in our inner (hat variables)

$$\hat{u} - 1 = \frac{\alpha}{R}\varepsilon^{-1}\frac{\partial\hat{u}}{\partial\hat{z}} = \left(\frac{\alpha}{s}\right)\frac{\partial\hat{u}}{\partial\hat{z}}. \tag{4.5}$$

Then using the inner boundary layer variables given by (4.4) and expanding $\hat{\bar{u}}, \hat{\bar{w}}$ and $\hat{\bar{p}}$ for small $(\varepsilon Re)^{-1}$ in the form

$$\hat{\bar{u}} = \hat{\bar{u}}_0 + \ldots, \quad \hat{\bar{w}} = \hat{\bar{w}}_0 + \ldots, \quad \hat{\bar{p}} = \hat{\bar{p}}_0 + \ldots,$$

we see that in a manner similar to the outer boundary layer, our inner boundary layer velocity field $\hat{\bar{u}}_0, \hat{\bar{w}}_0$ satisfies the boundary layer equations (see (3.9))

$$\frac{\partial^2\hat{\bar{u}}_0}{\partial\hat{\bar{z}}^2} = \hat{\bar{u}}_0\frac{\partial\hat{\bar{u}}_0}{\partial\hat{\bar{x}}} + \hat{\bar{w}}_0\frac{\partial\hat{\bar{u}}_0}{\partial\hat{\bar{z}}}, \quad \frac{\partial\hat{\bar{u}}_0}{\partial\hat{\bar{x}}} + \frac{\partial\hat{\bar{w}}_0}{\partial\hat{\bar{z}}} = 0, \tag{4.6}$$

where

$$\hat{\bar{u}}_0 \to 0 \quad \text{as} \quad \hat{\bar{z}} \to \infty, \tag{4.7}$$

and

$$\hat{\bar{w}}_0 = 0 \quad \text{on} \quad \hat{\bar{z}} = 0, \tag{4.8}$$

with the slip law (4.5) taking the form

$$\hat{\bar{u}}_0 - 1 = \left(\frac{\alpha}{s}\right)(\varepsilon^{-1}Re^{-1})^{-1/2}\frac{\partial\hat{\bar{u}}_0}{\partial\hat{\bar{z}}} \quad \text{on} \quad \hat{\bar{z}} = 0. \tag{4.9}$$

In order that the solution of (4.6) with boundary conditions (4.7)–(4.9) does not depend on Re we define the 'slip length' s so that

$$\left(\frac{\alpha}{s}\right)(\varepsilon^{-1}Re^{-1})^{-1/2} = 1, \tag{4.10}$$

https://doi.org/10.1017/S0022112097008112 Published online by Cambridge University Press

the boundary condition (4.9) then taking the form

$$\hat{\bar{u}}_0 - 1 = \frac{\partial \hat{\bar{u}}_0}{\partial \hat{\bar{z}}} \quad \text{on} \quad \hat{\bar{z}} = 0. \tag{4.11}$$

The relation (4.10) may be written as

$$\frac{\alpha}{s} = (\varepsilon^{-1} Re^{-1})^{1/2} = \left(\frac{\nu}{sU}\right)^{1/2} \tag{4.12}$$

giving the 'slip length' s as

$$s = \frac{\alpha^2 U}{\nu}. \tag{4.13}$$

The boundary layer equations (4.6) with boundary conditions (4.7), (4.8) and (4.11) possess a similarity solution for $\hat{\bar{x}} \to \infty$ when (4.11) is replaced by

$$\hat{\bar{u}}_0 = 1 \quad \text{on} \quad \hat{\bar{z}} = 0. \tag{4.14}$$

This solution, with $\hat{\bar{u}}_0, \hat{\bar{w}}_0$ of the form

$$\hat{\bar{u}}_0 = f_1(\hat{\bar{x}}^{-1/2}\hat{\bar{z}}), \quad \hat{\bar{w}}_0 = \hat{\bar{x}}^{-1/2} g_1(\hat{\bar{x}}^{-1/2}\hat{\bar{z}}) \tag{4.15}$$

is the same as that studied by Sakiadis (1961) (see § 3) for which

$$\hat{\bar{w}}_0 \sim -\tfrac{1}{2}\alpha^* \hat{\bar{x}}^{-1/2} \quad \text{as} \quad \hat{\bar{z}} \to \infty, \tag{4.16}$$

where α^* is given by (3.13). Also, for $\hat{\bar{x}} \to 0$, when (4.11) is replaced by

$$\frac{\partial \hat{\bar{u}}_0}{\partial \hat{\bar{z}}} = -1 \quad \text{on} \quad \hat{\bar{z}} = 0 \tag{4.17}$$

there is a similarity solution with $\hat{\bar{u}}_0, \hat{\bar{w}}_0$ of the form

$$\hat{\bar{u}}_0 = \hat{\bar{x}}^{1/3} f_2(\hat{\bar{x}}^{-1/3}\hat{\bar{z}}), \quad \hat{\bar{w}}_0 = \hat{\bar{x}}^{-1/3} g_2(\hat{\bar{x}}^{-1/3}\hat{\bar{z}}). \tag{4.18}$$

For a general value of $\hat{\bar{x}}$, the value of $\hat{\bar{w}}_0$ for $\hat{\bar{z}} \to \infty$ may be obtained by integrating the continuity equation in (4.6) as

$$\lim_{\hat{\bar{z}} \to \infty} \hat{\bar{w}}_0 = -\int_0^\infty \frac{\partial \hat{\bar{u}}_0}{\partial \hat{\bar{x}}} \, \mathrm{d}\hat{\bar{z}} \; (= F(\hat{\bar{x}}) \text{ say}), \tag{4.19}$$

where, by (4.16) and (4.18),

$$F(\hat{\bar{x}}) \sim A\hat{\bar{x}}^{-1/3} \quad \text{as} \quad \hat{\bar{x}} \to 0, \tag{4.20a}$$

$$F(\hat{\bar{x}}) \sim -\tfrac{1}{2}\alpha^* \hat{\bar{x}}^{-1/2} \quad \text{as} \quad \hat{\bar{x}} \to \infty. \tag{4.20b}$$

Thus we see by matching onto the inner inviscid region (using (4.4) and (4.6)), that the irrotational flow $\hat{\boldsymbol{u}} = (\hat{u}, 0, \hat{w})$ must satisfy

$$\hat{w} \sim (\varepsilon Re)^{-1/2} F(\hat{x}) \quad \text{on} \quad \hat{z} = 0. \tag{4.21}$$

This suggests that $\hat{\boldsymbol{u}} = (\hat{u}, 0, \hat{w})$ and pressure $\hat{p}$ should, for $(\varepsilon Re)^{-1} \to 0$, be expanded in a manner similar to the outer inviscid solution (see (3.15)) as

$$\hat{\boldsymbol{u}} = (\varepsilon Re)^{-1/2} \hat{\boldsymbol{u}}_1 + \ldots, \quad \hat{p} = (\varepsilon Re)^{-1} \hat{p}_1 + \ldots, \tag{4.22}$$

where $\hat{\boldsymbol{u}}_1$ is irrotational so that

$$\nabla \times \hat{\boldsymbol{u}}_1 = \boldsymbol{0}, \quad \nabla \cdot \hat{\boldsymbol{u}}_1 = 0 \tag{4.23}$$

https://doi.org/10.1017/S0022112097008112 Published online by Cambridge University Press

with

$$\hat{w}_1 = F(\hat{x}) \quad \text{on} \quad \hat{z} = 0 \tag{4.24}$$

and

$$\boldsymbol{n} \cdot \hat{\boldsymbol{u}}_1 = 0 \tag{4.25}$$

on the liquid interface. The normal stress boundary condition (3.20) at the liquid interface in our inner variables becomes

$$\hat{\kappa} = \tfrac{1}{2} Ca\ \varepsilon |\overline{\boldsymbol{u}}_1|^2 + O(\varepsilon) = \tfrac{1}{2} Ca\ (\varepsilon Re) |\hat{\boldsymbol{u}}|^2 + O(\varepsilon) = \tfrac{1}{2}\ Ca |\hat{\boldsymbol{u}}_1|^2 + O(\varepsilon), \tag{4.26}$$

where $\hat{\kappa} = \varepsilon \overline{\kappa}$ is the liquid interface curvature in inner variables. At order Ca^0, this boundary condition (4.26) gives $\hat{\kappa} = 0$, showing that the interface is planar at this order. Thus the interface may be written as

$$\phi = \theta_w + Ca\theta_1 + \ldots, \tag{4.27}$$

where θ_w is defined as the angle between the liquid interface and the solid surface at the contact line (at P). This angle θ_w, which will be called the microscopic contact angle is determined by the intermolecular forces acting very near the contact line between the molecules of the liquid and of the solid surface.

Thus at order Ca^0 the velocity field $\hat{\boldsymbol{u}}_1$ satisfies (4.23) to (4.25) with (4.25) applied on the Ca^0 position of the liquid interface (i.e. on the plane (4.27)). Thus $\boldsymbol{u}_1$ at this order is a function only of position $\hat{r}, \phi$ in the inner variables and of θ_w so that if we write

$$\hat{\boldsymbol{u}}_1 = \boldsymbol{G}(\hat{r}, \phi; \theta_w) \tag{4.28}$$

we see from the form of $F(\hat{x})$ as $\hat{x} \to \infty$ (see (4.20*b*)) that, as in § 3, $\hat{\boldsymbol{u}}_1$ for $\hat{r} \to \infty$ is given by (3.32) and (3.33) with $\hat{r}$ replacing $\bar{r}$. Also in a similar manner we see from the form of $F(\hat{x})$ as $\hat{x} \to 0$ (see (4.20*a*)) that, as $\hat{r} \to 0, \hat{\boldsymbol{u}}_1$ is proportional to $\hat{r}^{-1/3}$. Thus the liquid interface at order Ca^{+1} given by (4.26) is

$$\hat{\kappa} \equiv \frac{\mathrm{d}\theta_1}{\mathrm{d}\hat{r}} = \tfrac{1}{2}\ Ca\ |\ \boldsymbol{G}(\hat{r}, \phi; \theta_w)\ |^2, \tag{4.29}$$

where

$$\begin{aligned} |\ \boldsymbol{G}(\hat{r}, \theta_w; \theta_w)\ |^2 &\sim \tfrac{1}{4}\alpha^{*2}\hat{r}^{-1}\ \mathrm{cosec}^2 \tfrac{1}{2}\theta_w \quad \text{as} \quad \hat{r} \to \infty \\ &\sim \hat{r}^{-2/3} \quad \text{as} \quad \hat{r} \to 0. \end{aligned} \tag{4.30}$$

Equation (4.29) may be integrated to give the slope angle θ of the liquid interface as

$$\theta(\hat{r}) = \theta_w + \tfrac{1}{2} Ca \int_0^{\hat{r}} |\ \boldsymbol{G}(\hat{r}, \theta_w; \theta_w)\ |^2\ \mathrm{d}\hat{r} \tag{4.31}$$

where we note from (4.30) that the integral is convergent at its lower limit (so that it is unnecessary to examine the breakdown of the boundary layer solution close to $\hat{r} = 0$) and also that as $\hat{r} \to \infty$ the liquid interface has the asymptotic form

$$\theta(\hat{r}) = \theta_w + Ca \left\{ \tfrac{1}{8}\alpha^{*2} \mathrm{cosec}^2\ \tfrac{1}{2}\theta_w \ln \hat{r} + Q^*_{iv} + \ldots \right\}, \tag{4.32}$$

where the integration constant Q^*_{iv} depends only on θ_w. However it should be noted that if the slip length s had not been chosen in the manner given by (4.10) (and

https://doi.org/10.1017/S0022112097008112 Published online by Cambridge University Press

(4.13)) then Q_{iv}^* would not be a constant but would depend on the spreading velocity U (and on v and α)†.

From the above analysis of the situation where one has the particular slip model given by (4.5), we can see that for any realistic slip model (in which one has the no-slip condition for large $\hat{x}$) the interface shape will be given by (4.32) for $\hat{r} \to \infty$ although in general, for the constant Q_{iv}^* not to depend on the spreading velocity, it would require a suitable definition of the slip length s.

The slip model (considered by Huh & Mason 1977*b*) in which one has zero tangential stress on the liquid at the solid surface at distances from the contact line less than some distance s^* and no slip for distances greater than s^*, may be written in terms of the inner variables as

$$\left.\begin{aligned} \frac{\partial \hat{u}}{\partial \hat{z}} = 0 \quad \text{for} \quad 0 \leqslant \hat{x} < \frac{s^*}{s}, \\ \hat{u} = 1 \quad \text{for} \quad \frac{s^*}{s} \leqslant \hat{x} \end{aligned}\right\} \tag{4.33}$$

on the solid surface $\hat{z} = 0$. Then it is readily seen that to obtain the asymptotic form (4.32) of the liquid interface for $\hat{r} \to \infty$ in which Q_{iv}^* does not depend on the spreading velocity U would require

$$s = s^* \tag{4.34}$$

so that in this model at least the slip length would be independent of U.

For a more general type of the slip model (4.5) in which the difference Δu in tangential velocity between liquid and solid is

$$\Delta u = B \mid \text{shear gradient} \mid^p \tag{4.35}$$

where B and p are constants‡ ($p > 0$), one may, by arguments similar to that given above for the case $p = 1$, show that for Q_{iv}^* in (4.32) not to depend on the spreading velocity U, the slip length s must be chosen such that

$$s = v^{-1} U^{3-2/p} B^{2/p} \tag{4.36}$$

showing that as U increases, s will either increase or decrease according to whether p is greater than or less than $\frac{2}{3}$.

It is interesting to note that, for the situation considered by Cox (1986) where viscous forces dominate ($UR/v \ll 1$), the slip model (4.33) requires, for the quantity corresponding to Q_{iv}^* (see equation (4.13) in Cox 1986) not to depend on the spreading velocity U, that again

$$s = s^*. \tag{4.37}$$

However for slip model (4.35) one would require, for this viscous-dominated case ($UR/v \ll 1$), the slip length s to be

$$s = U^{1-1/p} B^{1/p} \tag{4.38}$$

showing that for this situation, as U increases, s will either increase or decrease according to whether p is greater than or less than unity. This result (4.38) for the slip

† This seems to be a relatively unimportant point since Q_{iv}^* can be incorporated into the scaling for $\hat{r}$ whatever its dependence on U, v and θ_w provided that these are given. The crucial results are clearly (4.31), which shows that the velocity singularity does not prevent the continuum model used from having a well-defined contact angle, and (4.17), which removes the integrated force singularity on the surface as the contact line is approached.

‡ Note that B will have dimensions of (velocity) $^{1-p}$ (length) ^{p}.

https://doi.org/10.1017/S0022112097008112 Published online by Cambridge University Press

length for the viscous situation is different from that required for the present inviscid situation (see (4.36)).

5. Matching with two and three regions

If the limit of $Ca \to 0$ with ε fixed and small is considered, the outer and inner solutions may be matched onto each other. Thus writing (4.32), the inner solution valid for $\hat{r} \to \infty$, in terms of outer variables, we obtain

$$\theta = \{\theta_w + \ldots\} + Ca\ \left\{\tfrac{1}{8}\alpha^{*2}\mathrm{cosec}^2\tfrac{1}{2}\ \theta_w(\ln\bar{r} + \ln\varepsilon^{-1}) + Q^*_{iv} + \ldots\right\} + \ldots \tag{5.1}$$

which when compared with the outer solution (3.39) valid for $\bar{r} \to 0$ with $\theta_m = \theta_{m0} + Ca\theta_{m1} + \ldots$, gives

$$\theta_{m0} = \theta_w, \quad \theta_{m1} = \tfrac{1}{8}\alpha^{*2}\mathrm{cosec}^2\tfrac{1}{2}\theta_w \ln\varepsilon^{-1} + Q^*_{iv} \tag{5.2}$$

with the terms in $\ln r$ automatically matching. Thus

$$\theta_m = \theta_w + Ca\ \left\{\tfrac{1}{8}\alpha^{*2}\mathrm{cosec}^2\tfrac{1}{2}\theta_w(\ln\varepsilon^{-1}) + Q^*_{iv}(\theta_w)\right\}. \tag{5.3}$$

This result (5.3) relates the unknown constant θ_m, the macroscopic contact angle, appearing in the outer region solution, to the spreading velocity U (involved in the definition of Ca) and to the microscopic contact angle θ_w. As mentioned in § 3, this macroscopic contact angle θ_m is considered as being determined by the asymptotic form (3.39) of the liquid interface shape as the contact line is approached in the outer region (i.e. as $\bar{r} \to 0$).

In a manner similar to the situation where viscous forces dominate (Cox 1986), it is seen that (5.3) is only valid for $Ca \to 0$, $\varepsilon \to 0$ if the quantity $Ca\ln(\varepsilon^{-1})$ also tends to zero. Under such a situation the interface is approximately planar near the contact line in the inner and outer regions. However when $Ca \to 0$, $\varepsilon \to 0$ with $Ca\ln(\varepsilon^{-1})$ of order unity, the result (5.3) is no longer valid since there is then no overlap of the inner and outer regions. It is then necessary to introduce a third region called the *intermediate* region which must exist between the inner and outer regions. This was done by Hocking & Rivers (1982) and Cox (1986) for the viscous flow situation ($UR/v \ll 1$). In the subsequent analysis we limit ourselves to this case ($Ca \to 0, \varepsilon \to 0$ with $Ca\ln(\varepsilon^{-1})$ of order unity) where the three regions are necessary.

6. Intermediate region

In the intermediate region (see figure 3), we use the same coordinates $(\tilde{X}, \phi)$ as for the viscous flow case (Cox 1986) with $\tilde{X}$ defined by

$$\tilde{X} = Ca\ln\bar{r}, \tag{6.1}$$

where

$$-Ca\ln(\varepsilon^{-1}) < \tilde{X} < 0. \tag{6.2}$$

Then it is seen that the end points $\tilde{X} = 0$ and $\tilde{X} = -Ca\ln(\varepsilon^{-1})$ correspond respectively to the outer region (with $\bar{r}$ of order unity) and the inner region (with $\hat{r}$ of order unity). Thus the intermediate-region expansion must be matched onto the outer region at $\tilde{X} = 0$ and onto the inner region at $\tilde{X} = -(Ca\ln(\varepsilon^{-1}))$. The velocity $\tilde{\boldsymbol{u}}$ and pressure $\tilde{p}$ in this intermediate region are defined by

$$\tilde{\boldsymbol{u}} = \bar{\boldsymbol{u}}, \quad \tilde{p} = \bar{p}. \tag{6.3}$$

https://doi.org/10.1017/S0022112097008112 Published online by Cambridge University Press

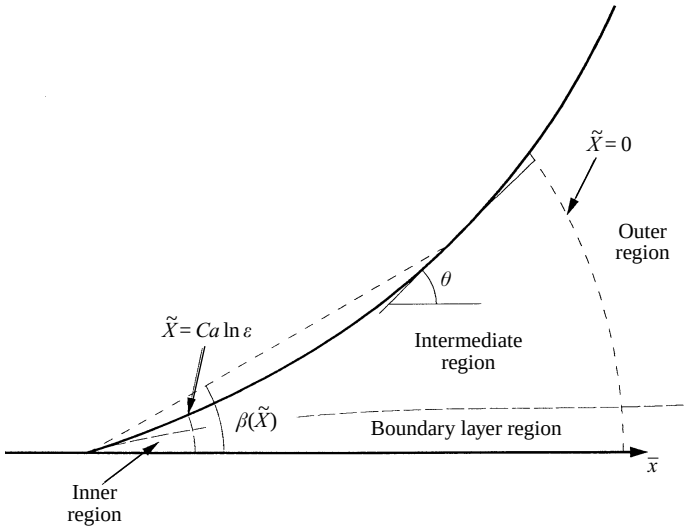


FIGURE 3. The intermediate region.

Since for any fixed value of $\tilde{X}(<0), \bar{r}$ is exponentially small for $Ca \to 0$, the flow is two-dimensional. Again as in both inner and outer regions we have irrotational flow except in a boundary layer at the solid surface. Also, since in this intermediate region the no-slip boundary condition applies at the solid surface with the irrotational flow outside the boundary layer (in the intermediate inviscid region) being the zero flow at order Ca^0, it follows, as in the outer region, that at order Ca^0 the boundary layer is that of Sakiadis (see § 3). Thus we see that in the intermediate inviscid region the velocity $\tilde{\boldsymbol{u}}$ is of order $Re^{-1/2}$ (and pressure $\tilde{p}$ of order Re^{-1}) with a flow into the boundary layer given by (3.14). Thus in the intermediate inviscid region we expand for large Re as

$$\tilde{\boldsymbol{u}} = Re^{-1/2}\tilde{\boldsymbol{u}}_1 + \ldots, \quad \tilde{p} = Re^{-1}\tilde{p}_1 + \ldots, \tag{6.4}$$

where $\tilde{\boldsymbol{u}}_1$ is irrotational so that

$$\nabla \times \tilde{\boldsymbol{u}}_1 = \boldsymbol{0}, \quad \nabla \cdot \tilde{\boldsymbol{u}}_1 = 0 \tag{6.5}$$

with the ϕ-component of $\tilde{\boldsymbol{u}}_1$ on $\phi = 0$ corresponding to the flow (3.14) into the boundary layer, i.e.

$$(\tilde{u}_1)_\phi = -\tfrac{1}{2}\alpha^* \bar{r}^{-1/2} \quad \text{on} \quad \phi = 0. \tag{6.6}$$

The zero normal velocity condition is

$$\boldsymbol{n} \cdot \tilde{\boldsymbol{u}}_1 = 0 \tag{6.7}$$

on the liquid interface (where $\boldsymbol{n}$ is a unit normal vector to that interface). Since $\tilde{\boldsymbol{u}}_1$ is two-dimensional, a stream function $\tilde{\psi}_1 = \overline{\psi}_1$ defined as in (3.27) may be used so that

$$\overline{\nabla}^2 \tilde{\psi}_1 = 0 \tag{6.8}$$

with the radial component $(\tilde{u}_1)_r$ and transverse component $(\tilde{u}_1)_\phi$ of $\tilde{\boldsymbol{u}}_1$ given by

$$(\tilde{u}_1)_r = \frac{1}{\bar{r}}\frac{\partial \tilde{\psi}_1}{\partial \phi}, \quad (\tilde{u}_1)_\phi = -\frac{\partial \tilde{\psi}_1}{\partial \bar{r}}. \tag{6.9}$$

https://doi.org/10.1017/S0022112097008112 Published online by Cambridge University Press

The boundary condition (6.6) suggests that in our intermediate inviscid region $\tilde{\psi}_1$ should be taken as

$$\tilde{\psi}_1 = \bar{r}^{1/2}\tilde{g}(\tilde{X}, \phi). \tag{6.10}$$

Substituting this expression for $\tilde{\psi}_1$ into (6.9), we see that the velocity components $(\tilde{u}_1)_r$ and $(\tilde{u}_1)_\phi$ are given are given in terms of our intermediate-region variables as

$$(\tilde{u}_1)_r = \bar{r}^{-1/2}\frac{\partial \tilde{g}}{\partial \phi}, \quad (\tilde{u}_1)_\phi = \bar{r}^{-1/2}\left(-\tfrac{1}{2}\tilde{g} - Ca\frac{\partial \tilde{g}}{\partial \tilde{X}}\right). \tag{6.11}$$

Likewise the equation (6.8) for $\tilde{\psi}_1$ becomes

$$\left(\frac{\partial^2 \tilde{g}}{\partial \phi^2} + \tfrac{1}{4}\tilde{g}\right) + Ca\frac{\partial \tilde{g}}{\partial \tilde{X}} + Ca^2\frac{\partial^2 \tilde{g}}{\partial \tilde{X}^2} = 0. \tag{6.12}$$

The boundary condition (6.6) on the solid surface $\phi = 0$ may, by using (6.11), be written as

$$\tilde{g} + 2Ca\,\frac{\partial \tilde{g}}{\partial \tilde{X}} = \alpha^* \quad \text{on} \quad \phi = 0 \tag{6.13}$$

which, when solved in terms of $\tilde{X}$, gives

$$\tilde{g} = \alpha^* + A\exp(-\tilde{X}/2Ca) \quad \text{on} \quad \phi = 0, \tag{6.14}$$

where A is a constant. This gives

$$\tilde{\psi}_1 = \alpha^*\bar{r}^{1/2} + A \quad \text{on} \quad \phi = 0 \tag{6.15}$$

and since the stream function as defined is arbitrary to within an added constant, A may be chosen to be zero. Thus the boundary condition (6.6) may written in the form

$$\tilde{g} = \alpha^* \quad \text{on} \quad \phi = 0. \tag{6.16}$$

In the same manner as for the viscous case, the liquid interface is taken as

$$\phi = \tilde{\beta}(\tilde{X}). \tag{6.17}$$

The fluid velocity component u_n (away from the liquid) normal to this interface is then found to be exactly

$$u_n = \left\{1 + \left(Ca\,\frac{\mathrm{d}\tilde{\beta}}{\mathrm{d}\tilde{X}}\right)^2\right\}^{-1/2}\left\{-\tfrac{1}{2}\tilde{g} - Ca\,\frac{\partial \tilde{g}}{\partial \tilde{X}} - Ca\,\frac{\mathrm{d}\tilde{\beta}}{\mathrm{d}\tilde{X}}\frac{\partial \tilde{g}}{\partial \phi}\right\}\bar{r}^{-1/2} \tag{6.18}$$

so that the condition of zero normal velocity at the interface gives

$$\tilde{g} + 2Ca\,\frac{\mathrm{d}\tilde{g}}{\mathrm{d}\tilde{X}} = 0 \quad \text{on} \quad \phi = \tilde{\beta}(\tilde{X}) \tag{6.19}$$

where

$$\frac{\mathrm{d}}{\mathrm{d}\tilde{X}} \equiv \frac{\partial}{\partial \tilde{X}} + \frac{\mathrm{d}\tilde{\beta}}{\mathrm{d}\tilde{X}}\frac{\partial}{\partial \phi}$$

is the total derivative with respect to $\tilde{X}$ along the interface. The solution of (6.19) is

$$\tilde{g} = A'\exp(-\tilde{X}/2Ca) \tag{6.20}$$

where A' is a constant. This corresponds to $\tilde{\psi}_1 = A'$ and since $\tilde{\psi}_1$ was taken to be zero on $\phi = 0$ as $\bar{r}^{1/2} \to 0$ in (6.15) and there is no fluid source at the contact line, it

https://doi.org/10.1017/S0022112097008112 Published online by Cambridge University Press

follows that $A' = 0$. Thus the boundary condition (6.19) becomes

$$\tilde{g} = 0 \quad \text{on} \quad \phi = \tilde{\beta}(\tilde{X}). \tag{6.21}$$

With the values of $(\tilde{u}_1)_r$ and $(\tilde{u}_1)_\phi$ given by (6.11), Bernoulli's equation (3.18) written in terms of the intermediate-region variables gives the value of $\tilde{p}_1$ in (6.4) as

$$\tilde{p}_1 = -\tfrac{1}{2}\bar{r}^{-1}\left\{\tfrac{1}{4}\tilde{g}^2 + \left(\frac{\partial\tilde{g}}{\partial\phi}\right)^2 + Ca\,\tilde{g}\frac{\partial\tilde{g}}{\partial\tilde{X}} + Ca^2\left(\frac{\partial\tilde{g}}{\partial\tilde{X}}\right)^2\right\}, \tag{6.22}$$

where the constant (and hydrostatic) term may be omitted since for any $\tilde{X}(<0)$ it will give an exponentially small fractional error of order $\bar{r}^{+1} = \exp(\tilde{X}/Ca)$ as $Ca \to 0$.

The curvature $\bar{\kappa}$ of the liquid interface given by (6.17) was determined by Cox (1986, equation (6.25)) as

$$\bar{\kappa} = Ca\,\bar{r}^{-1}\left\{1 + \left(Ca\,\frac{\mathrm{d}\tilde{\beta}}{\mathrm{d}\tilde{X}}\right)^2\right\}^{-3/2}\left\{\frac{\mathrm{d}\tilde{\beta}}{\mathrm{d}\tilde{X}} + Ca\,\frac{\mathrm{d}^2\tilde{\beta}}{\mathrm{d}\tilde{X}^2} + Ca^2\left(\frac{\mathrm{d}\tilde{\beta}}{\mathrm{d}\tilde{X}}\right)^3\right\}. \tag{6.23}$$

From the form of the equation (6.12) and boundary conditions (6.16) and (6.21) for $\tilde{g}$ it is seen that this quantity must be of the form

$$\tilde{g} = \tilde{g}_0 + Ca\tilde{g}_1 + \ldots, \tag{6.24}$$

where $\tilde{g}_0$ satisfies

$$\frac{\partial^2\tilde{g}_0}{\partial\phi^2} + \tfrac{1}{4}\tilde{g}_0 = 0 \tag{6.25}$$

with

$$\tilde{g}_0 = \alpha^* \quad \text{on} \quad \phi = 0, \tag{6.26}$$

$$\tilde{g}_0 = 0 \quad \text{on} \quad \phi = \tilde{\beta}(\tilde{X}) \tag{6.27}$$

whilst $\tilde{g}_1$ satisfies

$$\frac{\partial^2\tilde{g}_1}{\partial\phi^2} + \tfrac{1}{4}\tilde{g}_1 = -\frac{\partial\tilde{g}_0}{\partial\tilde{X}} \tag{6.28}$$

with

$$\tilde{g}_1 = 0 \quad \text{on} \quad \phi = 0 \quad \text{and on} \quad \phi = \tilde{\beta}(\tilde{X}). \tag{6.29}$$

The solution of (6.25)–(6.27) for $\tilde{g}_0$ is

$$\tilde{g}_0 = \alpha^*\left\{\cos\tfrac{1}{2}\phi - \cot\tfrac{1}{2}\tilde{\beta}(\tilde{X})\sin\tfrac{1}{2}\phi\right\} \tag{6.30}$$

so that (6.28) may be written as

$$\frac{\partial^2\tilde{g}_1}{\partial\phi^2} + \tfrac{1}{4}\tilde{g}_1 = -\alpha^*\left\{\frac{1}{2}\frac{\mathrm{d}\tilde{\beta}}{\mathrm{d}\tilde{X}}\mathrm{cosec}^2\tfrac{1}{2}\tilde{\beta}(\tilde{X})\sin\tfrac{1}{2}\phi\right\}. \tag{6.31}$$

With the boundary conditions (6.29), this possesses the solution

$$\tilde{g}_1 = \tfrac{1}{2}\alpha^*\frac{\mathrm{d}\tilde{\beta}}{\mathrm{d}\tilde{X}}\mathrm{cosec}^2\tfrac{1}{2}\tilde{\beta}\left\{\phi\cos\tfrac{1}{2}\phi - \tilde{\beta}\cot\tfrac{1}{2}\tilde{\beta}\sin\tfrac{1}{2}\phi\right\}. \tag{6.32}$$

If the value of $\tilde{g}$ given by (6.24) is substituted into (6.22) the pressure $\tilde{p}_1$ is obtained as

$$\tilde{p}_1 = -\tfrac{1}{2}\bar{r}^{-1}\left[\left\{\tfrac{1}{4}\tilde{g}_0^2 + \left(\frac{\partial\tilde{g}_0}{\partial\phi}\right)^2\right\} + Ca\left\{\tfrac{1}{2}\,\tilde{g}_0\tilde{g}_1 + 2\frac{\partial\tilde{g}_0}{\partial\phi}\frac{\partial\tilde{g}_1}{\partial\phi} + \tilde{g}_0\frac{\partial\tilde{g}_0}{\partial\tilde{X}}\right\} + \ldots\right] \tag{6.33}$$

https://doi.org/10.1017/S0022112097008112 Published online by Cambridge University Press

which, with the values of $\tilde{g}_0$ and $\tilde{g}_1$ given by (6.30) and (6.32) yields the pressure at the liquid interface $\phi = \tilde{\beta}(\tilde{X})$ as being

$$\tilde{p}_1 = -\tfrac{1}{2}\alpha^{*2}\bar{r}^{-1}\left[\left(\tfrac{1}{4}\mathrm{cosec}^2\tfrac{1}{2}\tilde{\beta}\right) + Ca\left(\frac{1}{4}\frac{\mathrm{d}\tilde{\beta}}{\mathrm{d}\tilde{X}}\mathrm{cosec}^4\tfrac{1}{2}\tilde{\beta}\right)(\tilde{\beta} - \sin\tilde{\beta}) + \ldots\right]. \tag{6.34}$$

The normal stress boundary condition (3.22) at the liquid interface

$$\bar{\kappa} = -Ca\ \tilde{p}_1 \quad \text{on} \quad \phi = \tilde{\beta}(\tilde{X})$$

may, by (6.23) and (6.34), now be written in terms of the intermediate-region variables as

$$\frac{\mathrm{d}\tilde{\beta}}{\mathrm{d}\tilde{X}} + Ca\ \frac{\mathrm{d}^2\tilde{\beta}}{\mathrm{d}\tilde{X}^2} = \tfrac{1}{8}\alpha^{*2}\left[\left(\mathrm{cosec}^2\tfrac{1}{2}\tilde{\beta}\right) + Ca\ \left\{\frac{\mathrm{d}\tilde{\beta}}{\mathrm{d}\tilde{X}}(\tilde{\beta} - \sin\tilde{\beta})\mathrm{cosec}^4\tfrac{1}{2}\tilde{\beta}\right\} + O(Ca^2)\right]. \tag{6.35}$$

Thus $\tilde{\beta}$ must be of the form

$$\tilde{\beta} = \tilde{\beta}_0 + Ca\ \tilde{\beta}_1(\tilde{X}) + \ldots \tag{6.36}$$

and this, when substituted into (6.35), gives at order Ca^0

$$\frac{\mathrm{d}\tilde{\beta}_0}{\mathrm{d}\tilde{X}} = \tfrac{1}{8}\alpha^{*2}\mathrm{cosec}^2\tfrac{1}{2}\tilde{\beta}_0 \tag{6.37}$$

and at order Ca^{+1}

$$\frac{\mathrm{d}\tilde{\beta}_1}{\mathrm{d}\tilde{X}} + \left(\tfrac{1}{8}\alpha^{*2}\mathrm{cosec}^3\tfrac{1}{2}\tilde{\beta}_0\cos\tfrac{1}{2}\beta_0\right)\tilde{\beta}_1 = -\frac{\mathrm{d}^2\tilde{\beta}_0}{\mathrm{d}\tilde{X}^2} + \tfrac{1}{8}\alpha^2\frac{\mathrm{d}\tilde{\beta}_0}{\mathrm{d}\tilde{X}}(\tilde{\beta}_0 - \sin\beta_0)\ \mathrm{cosec}^4\tfrac{1}{2}\tilde{\beta}_0. \tag{6.38}$$

The solution of (6.37) for $\tilde{\beta}_0$ is

$$\tilde{X} = g_{iv}(\tilde{\beta}_0) + K \tag{6.39}$$

where

$$g_{iv}(\tilde{\beta}_0) = 4\alpha^{*-2}(\tilde{\beta}_0 - \sin\tilde{\beta}_0) \tag{6.40}$$

and K is an arbitrary constant of integration.

If $\tilde{X}$ is eliminated from equations (6.37) and (6.38) and $\tilde{\beta}_1$ considered as a function of $\tilde{\beta}_0$, we obtain after a lengthy calculation

$$\tilde{\beta}_1 = \mathrm{cosec}^2\tfrac{1}{2}\tilde{\beta}_0\left\{\tfrac{1}{8}\alpha^{*2}h_{iv}(\tilde{\beta}_0) + L\right\}, \tag{6.41}$$

where

$$h_{iv}(\tilde{\beta}_0) = -2\ln\left(\sin\tfrac{1}{2}\tilde{\beta}_0\right) + 2\int_{\pi}^{\tilde{\beta}_0}\frac{\beta\mathrm{d}\beta}{1-\cos\beta} \tag{6.42}$$

and L is an arbitrary constant.

From (6.36), (6.39) and (6.41), it is seen that correct to an error of order Ca^{+2} the liquid interface may be written as

$$\tilde{X} = \{g_{iv}(\tilde{\beta}) + K\} - Ca\{h_{iv}(\tilde{\beta}) + 8\alpha^{*-2}L\} + \ldots. \tag{6.43}$$

Since the slope angle θ that the liquid interface makes with the solid surface is (see Cox 1986, equation (6.9))

$$\theta = \tilde{\beta} + \tan^{-1}\left(Ca\frac{\mathrm{d}\tilde{\beta}}{\mathrm{d}\tilde{X}}\right) \sim \tilde{\beta} + Ca\frac{\mathrm{d}\tilde{\beta}}{\mathrm{d}\tilde{X}} + O(Ca^2), \tag{6.44}$$

https://doi.org/10.1017/S0022112097008112 Published online by Cambridge University Press

it is seen that the interface shape given by (6.43) may be expressed alternatively as

$$\tilde{X} = \{g_{iv}(\theta) + K\} - Ca\{1 + h_{iv}(\theta) + 8\alpha^{*-2}L\} + O(Ca^2). \tag{6.45}$$

From the form (3.39) of the outer expansion as $\bar{r} \to 0$ we see that matching onto the intermediate expansion requires that

$$\theta = \left(\theta_m + \tfrac{1}{8}\alpha^{*2}\mathrm{cosec}^2\tfrac{1}{2}\theta_m\tilde{X} + \ldots\right) + o(Ca^{+1}) \tag{6.46}$$

as $\tilde{X} \to 0$ in the intermediate region. From (6.40) we see that (6.46) may be written, by expanding for small $\tilde{X}$ and Ca, as

$$g_{iv}(\theta) = \{g_{iv}(\theta_m) + \tilde{X} + \ldots\} + o(Ca^{+1})$$

or as

$$\tilde{X} = \{g_{iv}(\theta) - g_{iv}(\theta_m) + o(\tilde{X})\} + o(Ca^{+1}). \tag{6.47}$$

Thus comparing this with (6.45) and making use of (6.46), we see that K and L must be

$$K = -g_{iv}(\theta_m), \tag{6.48}$$

$$L = -\tfrac{1}{8}\alpha^{*2}(1 + h_{iv}(\theta_m)). \tag{6.49}$$

Substituting these values back into (6.45) we obtain the liquid interface shape in the intermediate region as

$$\tilde{X} = \{g_{iv}(\theta) - g_{iv}(\theta_m)\} - Ca\{h_{iv}(\theta) - h_{iv}(\theta_m)\} + O(Ca^2). \tag{6.50}$$

Since the intermediate-region solution must be matched onto the asymptotic form (4.32) of the inner solution at $\tilde{X} = -Ca\ln(\varepsilon^{-1})$ we write

$$\tilde{X} = -Ca\ln(\varepsilon^{-1}) + \tilde{Y} \tag{6.51}$$

so that $\tilde{Y} = Ca\ln\hat{r}$. Then in the intermediate region, (6.50) may be written

$$\tilde{Y} = \{Ca\ln\varepsilon^{-1} + g_{iv}(\theta - g_{iv}(\theta_m)\} - Ca\{h_{iv}(\theta) - h_{iv}(\theta_m)\} + O(Ca^2), \tag{6.52}$$

where we are assuming that $(Ca\ln\varepsilon^{-1})$ is of order unity.

Then for matching, (4.32) expressed in terms of $\tilde{Y}$, i.e. as

$$\theta \sim \left(\theta_w + \tfrac{1}{8}\alpha^{*2}\mathrm{cosec}^2\tfrac{1}{2}\theta_w\tilde{Y} + \ldots\right) + Ca(Q_i^* + \ldots) + \ldots, \tag{6.53}$$

must in the limit $\tilde{Y} \to 0$ be identical with (6.52). Proceeding as for matching onto the outer region, we observe that from (6.53)

$$g_{iv}(\theta) = \{g_{iv}(\theta_w) + \tilde{Y} + \ldots\} + Ca\left\{8\alpha^{*-2}\sin^2\tfrac{1}{2}\theta_w Q_{iv}^* + \ldots\right\} + \ldots$$

or

$$\tilde{Y} = \{g_{iv}(\theta) - g_{iv}(\theta_w)\} - Ca\left\{8\ \alpha^{*-2}\sin^2\tfrac{1}{2}\theta_w Q_{iv}^* + \ldots\right\} + \ldots. \tag{6.54}$$

Thus by matching (and noting from (6.53) that $\theta \sim \theta_w + \ldots$) we obtain

$$-g_{iv}(\theta_w) - Ca\ g'_{iv}(\theta_w)Q_{iv}^* = Ca\ \ln\varepsilon^{-1} - g_{iv}(\theta_m) - Cah_{iv}(\theta_w) + Ca\ h_{iv}(\theta_m) + O(Ca^2), \tag{6.55}$$

where g'_{iv} is the derivative of the function g_{iv}. This result (6.55) may be written in the form

$$Ca = \frac{g_{iv}(\theta_m) - g_{iv}(\theta_w)}{\ln\varepsilon^{-1} + h_{iv}(\theta_m) - h_{iv}(\theta_w) + g'_{iv}(\theta_w)Q_{iv}^*} + O\left(\frac{1}{\ln\varepsilon^{-1}}\right)^3 \tag{6.56}$$

https://doi.org/10.1017/S0022112097008112 Published online by Cambridge University Press

where, with the value of α^* given by (3.13), (see (6.40) and (6.42))

$$g_{iv}(\theta) = 1.53162(\theta - \sin\theta), \tag{6.57}$$

$$h_{iv}(\theta) = -2\ln(\sin\tfrac{1}{2}\theta) + 2\int_{\pi}^{\theta} \frac{\theta\,\mathrm{d}\theta}{(1-\cos\theta)}. \tag{6.58}$$

The result (6.56) gives the macroscopic contact angle θ_m in terms of the spreading velocity U (involved in the definition of Ca) and the microscopic contact angle θ_w where we have defined the macroscopic contact angle θ_m by the asymptotic form (3.39) of the interface shape as $\bar{r} \to 0$ in the outer region. Note that (3.39) may also be written in the form

$$\theta \sim (\theta_m + \ldots) + Ca\{(g_{iv}'(\theta_m))^{-1}\ln\bar{r} + o(\bar{r}^0)\} + \ldots. \tag{6.59}$$

The quantity Q_{iv}^* in (6.56) depends only on θ_w and the assumed slip law model at the solid surface.

These results, valid for the present situation ($\varepsilon Re \gg 1$) for *advancing* contact lines in which inertia effects dominate, are very similar to the analogous results (Cox (1986) equations (4.14), (3.21), (7.11) and (7.21)) for viscous flow ($Re \ll 1$) for both *advancing* and *receding* contact lines. These latter results (with some minor changes in notation) give

$$Ca = \frac{g_v(\theta_m) - g_v(\theta_w)}{\ln\varepsilon^{-1} + g_v'(\theta_w)\,Q_v^*} + O\left(\frac{1}{\ln\varepsilon^{-1}}\right)^3, \tag{6.60}$$

where $g_v(\theta)$ is the function

$$g_v(\theta) = \int_0^{\theta} \frac{\mathrm{d}\theta}{f_v(\theta)}, \tag{6.61}$$

where

$$f_v(\theta) = \frac{2\sin\theta[\lambda^2(\theta^2 - \sin^2\theta) + 2\lambda\{\theta(\pi-\theta) + \sin^2\theta\} + \{(\pi-\theta)^2 - \sin^2\theta\}]}{\lambda(\theta^2 - \sin^2\theta)\{(\pi-\theta) + \sin\theta\cos\theta\} + \{(\pi-\theta)^2 - \sin^2\theta\}(\theta - \sin\theta\cos\theta)} \tag{6.62}$$

for a fluid of viscosity μ displacing one of viscosity $\lambda\mu$. Here (6.60) relates the macroscopic contact angle θ_m to the spreading velocity U, the microscopic contact angle θ_w and the viscosity ratio λ. Again the macroscopic contact angle θ_m is defined by the asymptotic form as $\bar{r} \to 0$ of the interface shape in the outer region, i.e. by

$$\theta \sim (\theta_m + \ldots) + Ca\{(g_v'(\theta_m))^{-1}\ln\bar{r} + o(\bar{r}^0)\} + \ldots. \tag{6.63}$$

The quantity Q_v^* in (6.60), like Q_{iv}^*, depends only on θ_w and the assumed slip law model at the solid surface. Thus the results for our present inviscid flow ($\varepsilon Re \gg 1$) for advancing contact lines are essentially the same as for viscous flow ($Re \ll 1$) except that the function $g_v(\theta)$ is replaced by $g_{iv}(\theta)$ with additional terms involving a function $h_{iv}(\theta)$ appearing in (6.56).

7. Discussion of inviscid results

Since our result (6.56) for the macroscopic contact angle θ_m is valid for $Ca \to 0$ and $\varepsilon \to 0$ with $Ca\ln\varepsilon^{-1}$ of order unity, the values of θ_m obtained from (6.56) can differ from the microscopic contact angle θ_w by an amount of order unity (as was also true for the viscous result (6.60)). However if we consider the result (6.56) (or

https://doi.org/10.1017/S0022112097008112 Published online by Cambridge University Press

the equivalent result (6.55)) for the situation $Ca \to 0$ with ε fixed and small so that $Ca \ln \varepsilon^{-1} \to 0$, we see that at order Ca^0, θ_m is equal to θ_w. Thus

$$\theta_m = \theta_w + Ca\ \theta_1 + O(Ca^2)$$

which when substituted into (6.53) yields at order Ca^{+1}

$$\theta_1 = Q^*_{iv} + \frac{\ln \varepsilon}{g'_{iv}(\theta_w)}$$

giving, with g_{iv} defined by (6.57),

$$\theta_m = \theta_w + Ca \left\{ \tfrac{1}{8}\alpha^{*2} \mathrm{cosec}^2 \tfrac{1}{2}\theta_w (\ln \varepsilon^{-1}) + Q^*_{iv} \right\} + \ldots$$

which is identical to the result (5.3) valid for this situation obtained using two (inner and outer) rather than three (inner, intermediate and outer) regions of expansion.

In deriving our result (6.56) for the macroscopic contact angle θ_m, it was assumed that in the inviscid region outside the boundary layer (whether within the inner, intermediate or outer regions), there was zero flow at order Re^0. However if at this order there is a flow (produced for example by boundaries within the outer region having normal components of velocity) it must be a velocity field which behaves like $\bar{r}^{(2n\pi/\theta_m - 1)}$ as $\bar{r} \to 0$ where n is a positive integer (if the flow is irrotational) or possibly like $\bar{r}^{+1}$ (if the flow possesses vorticity)†. In either case this gives a velocity which tends to zero as the contact line is approached. However a non-zero pressure gradient in the $\bar{x}$-direction is produced at the solid wall (obtained by using Bernoulli's equation) which is proportional to $\bar{x}^{(4n\pi/\theta_m - 3)}$ (due to the irrotational velocity field) or to $\bar{x}^{+1}$ (if the flow possesses vorticity). This pressure gradient would then appear as an additional term in the boundary layer equations (3.9) but would have no effect on the boundary layer in the limit $\bar{x} \to 0$. Thus we see that the conditions (*e*) and (*h*) mentioned in § 2 for the validity of the present theory may be removed. This also implies that in the inner and intermediate regions (and outer region $\bar{r} \to 0$), the condition (*f*) of § 2 of no boundary layer separation is satisfied (there being negligible pressure gradient along the boundary layer).

The condition (*g*) in § 2 that the boundary layer does not become turbulent is almost certainly well satisfied within the inner region since for validity of the theory $Ca \ll 1$ implying that the spreading velocity U is much smaller than σ/μ. This would give the Reynolds number for the boundary layer based on the slip length s as smaller than $\sigma s/\mu\nu$ which would be almost certainly, for all fluids, very much smaller than the value of 10^5–10^6 required for the boundary layer to be turbulent. It is possible, however, that the Reynolds number (smaller than $\sigma R/\mu\nu$) for the boundary layer in the outer region may be high enough for the boundary layer there to be turbulent. If this is the case all that is necessary is to define θ_m from the interface shape (6.59) at smaller distances from the contact line where the boundary layer is known to be laminar.

The functions $g_{iv}(\theta)$ and $h_{iv}(\theta)$ given by (6.57) and (6.58), which are required for using (6.56), have been plotted in figure 4 from which it is observed that as θ increases from 0 to π, $g_{iv}(\theta)$ increases monotonically from zero to a value $4\pi\alpha^{*-2} (= 4.8117)$

† The arguments behind these deductions seem to be: for the irrotational case, any solution of (6.8) will have a leading term for $\tilde{\psi}$ of separable form $\bar{r}^m \exp(\mathrm{i}m\theta)$, which leads to $m = 2n\pi/\theta_m$ if it is required that $\tilde{\psi}$ has the same constant value on $\theta = 0$ and $\theta = \theta_m$; for the case with vorticity the hypothesis that the vorticity tends to a constant in a steady flow leads to a velocity field behaving as $\bar{r}$ near $\bar{r} = 0$.

https://doi.org/10.1017/S0022112097008112 Published online by Cambridge University Press

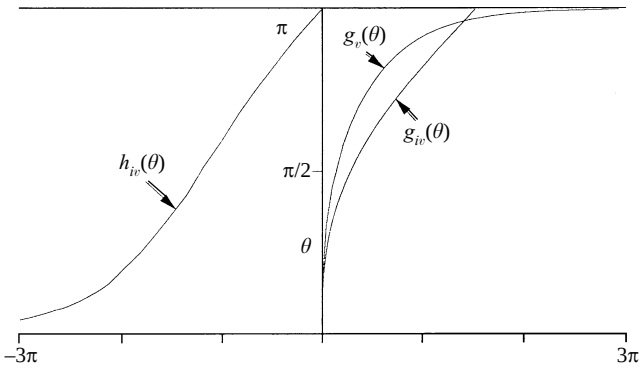


FIGURE 4. The functions $g_{iv}(\theta)$ and $h_{iv}(\theta)$ (given by (6.57) and (6.58)) and also $g_v(\theta)$ (given by (7.10)).

with asymptotic values readily shown to be

$$g_{iv} \sim \tfrac{2}{3}\alpha^{*-2}\theta^3 + \ldots \quad \text{as} \quad \theta \to 0 \tag{7.1}$$

$$\sim 4\pi\alpha^{*-2} - 8\alpha^{*-2}(\pi - \theta) + \ldots \quad \text{as} \quad \theta \to \pi. \tag{7.2}$$

Also h_{iv} increases monotonically from $-\infty$ at $\theta = 0$ to zero at $\theta = \pi$ with asymptotic values

$$h_{iv} \sim 2\ln\theta + \ldots \quad \text{as} \quad \theta \to 0 \tag{7.3}$$

$$\sim -\pi(\pi - \theta) + \tfrac{3}{4}(\pi - \theta)^2 + \ldots \quad \text{as} \quad \theta \to \pi. \tag{7.4}$$

Our result (6.55) for the advancing macroscopic contact angle θ_m may be put in a simpler, but more approximate form, by neglecting terms of order Ca^{+1} (but retaining the term $Ca\ln\varepsilon^{-1}$ since it is assumed to be of order unity) to obtain

$$g_{iv}(\theta_m) = g_{iv}(\theta_w) + Ca\ln\varepsilon^{-1} + O\left(\frac{1}{\ln\varepsilon^{-1}}\right) \tag{7.5}$$

or

$$Ca = \frac{g_{iv}(\theta_m) - g_{iv}(\theta_w)}{\ln\varepsilon^{-1}} + O\left(\frac{1}{\ln\varepsilon^{-1}}\right)^2, \tag{7.6}$$

where $g_{iv}(\theta)$ is given by (6.57).

The advantage in using the result (7.6) (or (7.5)) rather than (6.56) (or (6.55)) is that one does not have to calculate the quantity Q^*_{iv} which would involve the derivation of the flow field in the inner region for the particular slip model chosen. In fact the result (7.6), as written, is independent of the slip model used (or of any other mechanism which might get rid of the flow singularity at the contact line) although it should be noted that the slip length s, used in the definition of ε, may depend on the spreading velocity U in a manner dependent on the slip model which is chosen. Also the use of the result (7.5) (or (7.6)) is very straightforward with θ_m being obtained directly from the plot of θ versus g_{iv} (see figure 4) in a simple graphical procedure. Thus, as shown in figure 5, from the known value of the microscopic contact angle θ_w, the value of $g_{iv}(\theta_w)$ may be read off. Then by moving along the abscissa an amount $(Ca\ln\varepsilon^{-1})$ to the right the value of $g_{iv}(\theta_m)$ is obtained (see equation (7.5)), the value of θ_m then being read off on the ordinate.

From (7.5) and the form of $g_{iv}(\theta)$ shown in figure 5 it is observed that for any given microscopic contact angle θ_w the macroscopic contact angle θ_m increases

https://doi.org/10.1017/S0022112097008112 Published online by Cambridge University Press

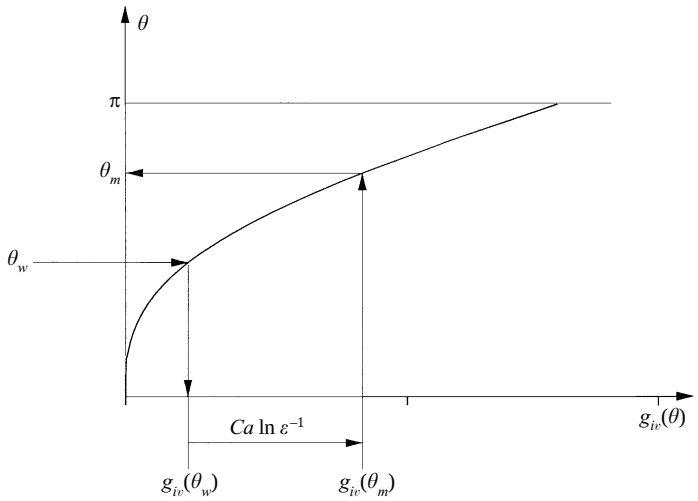


FIGURE 5. Graphical procedure for the calculation of θ_m.

monotonically with capillary number Ca (and hence with spreading velocity U) for an advancing contact line with a solution only existing up to a critical value Ca_{max} of the capillary number for which the macroscopic contact angle has the value of 180°. This value Ca_{max} is, by (7.5),

$$Ca_{max} = \frac{4\pi\alpha^{*-2} - g_{iv}(\theta_w)}{\ln \varepsilon^{-1}} \tag{7.7}$$

giving a maximum spreading velocity U_{max} of

$$U_{max} = \frac{\sigma}{\mu}\left(\frac{4\pi\alpha^{-2} - g_{iv}(\theta_w)}{\ln \varepsilon^{-1}}\right). \tag{7.8}$$

It is uncertain what happens in our present situation of $\varepsilon Re \gg 1$ if one physically imposes a spreading velocity greater than U_{max}. It seems that there is no steady shape of the interface possible. In the viscous situation of $Re \ll 1$ discussed by Cox (1986) a similar situation was predicted with the macroscopic contact angle θ_m increasing monotonically with Ca and obtaining a value of 180° at a critical capillary number (except for the case of an advancing contact line with a pair of immiscible fluids with a viscosity ratio $\lambda = 0$). For such a situation it is known experimentally that the liquid ahead of the contact line can be entrained as a film (or drops) beneath the other liquid behind the contact line (Invararity 1969; Burley & Brady 1973; Burley & Kennedy 1976; Kennedy & Burley 1977).

In a manner similar to the way in which the result (6.56) for the macroscopic contact angle for the present inviscid situation ($\varepsilon Re \gg 1$) may be approximated by (7.6), so also may the result (6.60) for the viscous situation (Cox 1986) be approximated by

$$Ca = \frac{g_v(\theta_m) - g_v(\theta_w)}{\ln \varepsilon^{-1}} + O\left(\frac{1}{\ln \varepsilon^{-1}}\right)^2, \tag{7.9}$$

where $g_v(\theta)$ is given by (6.61) and (6.62). As pointed out by Cox (1986), the value of θ_m may be obtained directly from the graph of θ versus $g_v(\theta)$ for a particular viscosity ratio λ in the same manner as for the inviscid case as shown in figure 5.

Thus for a single fluid advancing (into a vacuum) we see that the macroscopic

https://doi.org/10.1017/S0022112097008112 Published online by Cambridge University Press

contact angle θ_m is determined by (7.6) with $g_{iv}(\theta)$ given by (6.57) for the inviscid case $\varepsilon Re \gg 1$ and by (7.9) with $g_v(\theta)$ given by (6.61) and (6.62) with $\lambda = 0$, i.e. by

$$g_v(\theta) = \int_0^\theta \frac{(\theta - \sin\theta\cos\theta)}{2\sin\theta}\,\mathrm{d}\theta \tag{7.10}$$

for the viscous case $Re \ll 1$. The graph of θ versus $g_v(\theta)$ given by (7.10) is shown in figure 4.

Whilst it is easy to find examples of slowly spreading viscous liquids for which $Re \ll 1$ (for which one has a viscous situation), it requires a very inviscid fast spreading liquid for our present inviscid situation requiring $\varepsilon Re \gg 1$. However it can occur even for an advancing contact line for which the capillary number must be less than Ca_{max} given by (7.7). If we have, for example, water as the liquid with $\theta_w = 0°$, $s = 5 \times 10^{-5}$ cm and $R = 10^{-1}$ cm (giving $\varepsilon = 5 \times 10^{-4}$) then, by (7.7), $Ca_{max} = 0.63$ giving a maximum spreading velocity of 44 m s^{-1}. With such a velocity, εRe has a value of approximately 22.

However for water spreading at a lower speed or for a more viscous fluid one could have the situation in which one had neither the inviscid situation (with $\varepsilon Re \gg 1$) nor the viscous situation (with $Re \ll 1$). Such intermediate situations will examined in the following section.

8. Solution for general Reynolds number

In our present theory (given in §§ 2–6) we have examined inviscid spreading of a single liquid with $\varepsilon Re \gg 1$, by making an expansion in the capillary number Ca (correct to order Ca^{+1}) which had been assumed small. In doing this the quantity $(Ca \ln \varepsilon^{-1})$ was taken to be small or of order unity (there then being three regions of expansion). Cox (1986) examined viscous spreading with $Re \ll 1$ of one immiscible fluid displacing another. This was also done by making an expansion in the capillary number Ca (correct to order Ca^{+1}) with $Ca \ln \varepsilon^{-1}$ of order unity.

The results for both $\varepsilon Re \gg 1$ (or $Re \gg \varepsilon^{-1}$) and $Re \ll 1$ for the advancing of a single liquid in the more approximate form (correct to order Ca^0) have been given at the end of § 7. We now examine the more general situation

$$1 \ll Re \ll \varepsilon^{-1} \tag{8.1}$$

in which viscous effects dominate in the intermediate region as one approaches the inner region but the flow is inviscid (apart from the boundary layer on the solid surface) in the intermediate region as one approaches the outer region. This will be done also by making an expansion in the capillary number Ca with Re held fixed (and satisfying (8.1)) and with $(Ca \ln \varepsilon^{-1})$ assumed to be of order unity (so that one still has an inner, an intermediate and an outer region of expansion). However, for simplicity we only consider terms of order Ca^0, neglecting terms of order Ca^{+1}.

If we let

$$\tilde{X}^* = Ca \ln Re^{-1} \tag{8.2}$$

then $\tilde{X} = \tilde{X}^*$ is within the intermediate region since from the assumptions made

$$-Ca \ln \varepsilon^{-1} < \tilde{X}^* < 0. \tag{8.3}$$

In fact $\tilde{X} = \tilde{X}^*$ corresponds to a value of $\bar{r} = Re^{-1}$ and hence to radial distances r of order ν/U for which inertia and viscous effects are of the same order with rU/ν of order unity. Then we note that if we define a new independent variable r^* as radial

https://doi.org/10.1017/S0022112097008112 Published online by Cambridge University Press

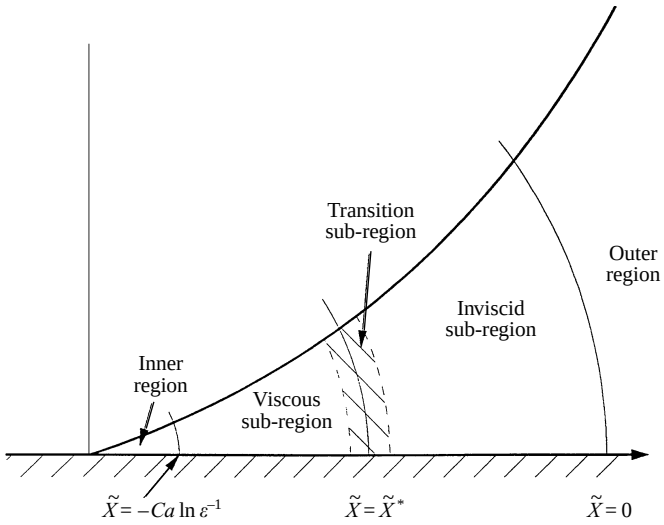


FIGURE 6. The sub-division of the intermediate region.

distance r from the contact line made dimensionless by the lengthscale ν/U so that

$$r^* = \frac{rU}{\nu} = Re\ \bar{r} \tag{8.4}$$

then

$$\tilde{X} - \tilde{X}^* = Ca \ln r^* \tag{8.5}$$

or

$$r^* = \exp\{Ca^{-1}(\tilde{X} - \tilde{X}^*)\}. \tag{8.6}$$

The intermediate region must now be subdivided into three subregions† as illustrated in figure 6, these being:

(a) A viscous sub-region in which $\tilde{X}$ satisfies

$$-Ca \ln \varepsilon^{-1} < \tilde{X} < \tilde{X}^* \tag{8.7}$$

with $\tilde{X}, \phi$ being used as independent variables (with velocity $\tilde{\boldsymbol{u}} = \bar{\boldsymbol{u}}$ and pressure $\tilde{p} = \bar{p}$). Throughout this region $rU/\nu = r^*$ is, by (8.6), exponentially small as $Ca \to 0$, so that the flow within this sub-region is viscous-dominated with the velocity and pressure satisfying the Stokes equations. This flow must be matched onto the viscous dominated flow in the inner region as $\tilde{X} \to -Ca \ln \varepsilon^{-1}$ from above.

(b) An inviscid sub-region in which $\tilde{X}$ satisfies

$$\tilde{X}^* < \tilde{X} < 0 \tag{8.8}$$

with $\tilde{X}, \phi$ again being used as independent variables (with velocity $\tilde{\boldsymbol{u}} = \bar{\boldsymbol{u}}$ and pressure $\tilde{p} = \bar{p}$). Throughout this sub-region $rU/\mu = r^*$ is, by (8.6), exponentially large as $Ca \to 0$, so that we have (for an advancing contact line) a high Reynolds number flow consisting of an irrotational flow with a boundary layer at the solid surface (as for the flow discussed in § 6). This flow must be matched onto the irrotational flow (and boundary layer) in the outer region (see § 3) as $\tilde{X} \to 0$ from below.

† Because $\tilde{X}$ already involves a logarithm, it seems reasonable to use $<$ instead of $\ll$ to define overlapping regions.

https://doi.org/10.1017/S0022112097008112 Published online by Cambridge University Press

(*c*) A transition sub-region at $\tilde{X} = \tilde{X}^* + O(Ca)$ in which r^*, ϕ are used as independent variables (with velocity $\tilde{\boldsymbol{u}}^* = \bar{\boldsymbol{u}}$ and pressure $\tilde{p}^* = \bar{p}$). In this sub-region where viscous and inertia effects are of the same order, we require that as $r^* \to 0$, the solution matches onto the viscous subregion with $\tilde{X} \to \tilde{X}^*$ from below and as $r^* \to \infty$, the solution matches onto the inviscid sub-region with $\tilde{X} \to \tilde{X}^*$ from above. In this transition sub-region, it may be readily shown that $\tilde{\boldsymbol{u}}^*, \tilde{p}^*$ satisfy the full steady Navier–Stokes equations

$$\left.\begin{aligned} \tilde{\nabla}^{*2}\tilde{\boldsymbol{u}}^* - \tilde{\nabla}^*\tilde{p}^* &= \tilde{\boldsymbol{u}}^* \cdot \tilde{\nabla}^*\tilde{\boldsymbol{u}}^*, \\ \tilde{\nabla}^* \cdot \tilde{\boldsymbol{u}}^* &= 0, \end{aligned}\right\} \tag{8.9}$$

with the boundary conditions

$$(\tilde{u}^*)_r = +1, \quad (\tilde{u}^*)_\phi = 0 \tag{8.10}$$

on $\phi = 0$ and

$$\tilde{u}_i^* n_i = 0, \quad t_i \tilde{\sigma}_{ij}^* n_j = 0 \tag{8.11}$$

on the liquid interface, where $(\tilde{u}^*)_r$ and $(\tilde{u}^*)_\phi$ are the radial and transverse components of $\tilde{\boldsymbol{u}}^*, \tilde{\sigma}_{ij}^*$ is the stress tensor and where $\boldsymbol{n}$ and $\boldsymbol{t}$ are unit normal and unit tangent respectively to the liquid interface. In addition, the normal stress boundary condition on the liquid interface may be written as

$$\tilde{\kappa}^* = Ca(n_i\ \tilde{\sigma}_{ij}^*\ n_j), \tag{8.12}$$

where $\tilde{\kappa}^*$ is the interface curvature made dimensionless by the lengthscale v/U (i.e. the lengthscale relevant to this transition region). Since for any particular liquid interface shape the solution of (8.9) with boundary conditions (8.10) and (8.11) must give a value of $\tilde{\sigma}_{ij}^*$ of order unity, the normal stress boundary condition (8.12) shows that the curvature $\tilde{\kappa}^*$ is of order Ca^{+1}. Thus the liquid interface shape must, as an expansion in Ca, be of the form

$$\theta = \theta^* + Ca\theta_1^* + \ldots, \tag{8.13}$$

where θ^* is a constant (but θ_1^* a function of $\tilde{r}^*$).

For an advancing contact line, we see that as $r^* \to \infty$ in the transition sub-region, we approach an inviscid flow situation in which we have an irrotational flow with a boundary layer at the solid surface. This is a situation similar to that for the outer region discussed in § 4 and we may obtain as $r^* \to \infty$

$$\theta \sim \theta^* + Ca\ \{(g_{iv}'(\theta^*))^{-1} \ln r^* + \ldots\}. \tag{8.14}$$

As $r^* \to 0$ in the transition sub-region we approach a viscous Stokes flow and following an analysis similar to that for the outer region for the viscous case (see Cox 1986, equation (3.28)) we may obtain as $r^* \to 0$

$$\theta \sim \theta^* + Ca\{(g_v'(\theta^*))^{-1} \ln r^* + \ldots\}. \tag{8.15}$$

Thus, by (8.14), we see that for matching onto the inviscid sub-region we require that as $\tilde{X} \to \tilde{X}^*$ from above

$$\theta \sim \{\theta^* + (g_{iv}'(\theta^*))^{-1}(\tilde{X} - \tilde{X}^*) + \ldots\} + O(Ca) \tag{8.16}$$

in the inviscid sub-region. Also, by (8.15) we see that in a similar manner we require that as $\tilde{X} \to \tilde{X}^*$ from below

$$\theta \sim \{\theta^* - (g_v'(\theta^*))^{-1}(\tilde{X}^* - \tilde{X}) + \ldots\} + O(Ca). \tag{8.17}$$

https://doi.org/10.1017/S0022112097008112 Published online by Cambridge University Press

Since the flow in the outer region is inertia dominated, we have the same solution there as obtained in § 3. This when matched onto the inviscid sub-region requires that as $\tilde{X} \to 0$ (see (6.44))

$$\theta \sim \{\theta_m + (g_{iv}'(\theta_m))^{-1}\tilde{X} + \ldots\} + O(Ca), \tag{8.18}$$

where θ_m is the same macroscopic contact angle as before (defined by the relation (6.63) for the liquid interface shape in the outer region). In the inner region where the flow satisfies the Stokes equations, we obtain (see Cox 1986, equation (4.14)) the interface shape for $\hat{r} \to \infty$ as

$$\theta \sim (\theta_w + \ldots) + Ca\{(g_v'(\theta_w))^{-1}\ln\hat{r} + Q_v^* + \ldots\} + \ldots \tag{8.19}$$

so that by matching onto the viscous sub-region we see that we require as $\tilde{X} \to -(Ca\ln\varepsilon^{-1})$

$$\theta \sim \{\theta_w + (g_v'(\theta_w))^{-1}\tilde{Y} + \ldots\} + O(Ca) \tag{8.20}$$

where $\tilde{Y} = \tilde{X} + Ca\ln\varepsilon^{-1}$ as in (6.51).

In the inviscid sub-region, the interface shape is that given by (6.45) which at order Ca^0 is

$$\tilde{X} = g_{iv}(\theta) + K_{iv}, \tag{8.21}$$

where K_{iv} is a constant. Applying the boundary conditions (8.16) for $\tilde{X} \to \tilde{X}^*$ from above and (8.18) for $\tilde{X} \to 0$ from below, we obtain

$$Ca\ln(Re) = g_{iv}(\theta_m) - g_{iv}(\theta^*). \tag{8.22}$$

Likewise in the viscous sub-region, the interface shape was obtained by Cox (1986) (see his equation (7.10)) which at order Ca^0 may be written

$$\tilde{X} = g_v(\theta) + K_v, \tag{8.23}$$

where K_v is a constant. Then by applying the boundary conditions (8.17) for $\tilde{X} \to \tilde{X}^*$ from below and (8.20) as $\tilde{X} \to -(Ca\ln\varepsilon^{-1})$ from above (or $\tilde{Y} \to 0$ from above), we obtain

$$Ca\ln(\varepsilon^{-1}Re^{-1}) = g_v(\theta^*) - g_v(\theta_w)\ . \tag{8.24}$$

Thus, for an advancing liquid, the macroscopic contact angle θ_m (defined by the asymptotic form (6.63) of the interface in the outer region) may be obtained by first deriving θ^* from (8.24) or graphically from $g_v(\theta)$ (shown in figure 4) in a manner similar to that shown in figure 5 (for (7.6)) with $\varepsilon Re(\ll 1)$ replacing ε (as if slip length s were replaced by sRU/v). Then θ_m is obtained from (8.22) or graphically from $g_{iv}(\theta)$ (shown in figure 5) with $Re^{-1}(\ll 1)$ replacing ε (as if slip length s were replaced by v/U).

While the results (8.22) and (8.24) determine the macroscopic contact angle for an advancing contact line for Reynolds number Re in the range given by (8.1) we note that if we substitute $Re = 1$ into these results, (8.22) gives $\theta^* = \theta_m$ with (8.24) then giving exactly the result (7.9) for the viscous case $Re \ll 1$) examined by Cox (1986). Likewise if we substitute $Re = \varepsilon^{-1}$ into the results, (8.24) gives $\theta^* = \theta_w$ with (8.22) giving exactly the result (7.6) for the inviscid case examined in §§ 2–6. Thus one may use (7.9) for $Re \leqslant 1$, (8.22) and (8.24) for $1 \leqslant Re \leqslant \varepsilon^{-1}$ and (7.6) for $\varepsilon^{-1} \leqslant Re$.

9. Discussion of results for general Reynolds number

The various results we have obtained in the previous sections for the macroscopic contact angle for contact lines and for various ranges of Reynolds number have been

https://doi.org/10.1017/S0022112097008112 Published online by Cambridge University Press

Advancing or receding contact line	Range of Re	Form of interface as $\bar{r} \to 0$ (Definition of θ_m)	Equation for θ_m
Advancing	$Re \leqslant 1$	(6.63)	(7.9)
Advancing	$1 \leqslant Re \leqslant \varepsilon^{-1}$	(6.59) (for $r > v/U$)	(8.22) & (8.24)
Advancing	$\varepsilon^{-1} \leqslant Re$	(6.59)	(7.6)

TABLE 1. Equations determining macroscopic contact angle θ_m.

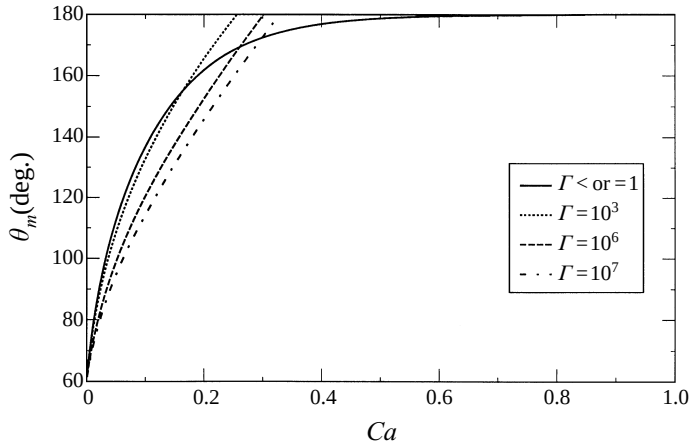


FIGURE 7. The macroscopic contact angle θ_m for an advancing contact line as a function of Ca for various values of Γ for $\theta_w = 60^\circ$ and $\varepsilon = 10^{-6}$.

listed in table 1. All these results give the macroscopic contact angle θ_m as a function of the microscopic contact angle θ_w, the capillary number Ca ($\ll 1$), the Reynolds number Re and the slip length ratio ε ($\ll 1$). In plotting graphically the results for any particular example it is more convenient to consider instead the macroscopic contact angle θ_m as a function of θ_w, Ca, Γ and ε where Γ is defined as

$$\Gamma \equiv \frac{Re}{Ca} \equiv \frac{R\sigma}{\mu v} \tag{9.1}$$

so that it is then only the parameter Ca that involves the spreading velocity U. Note that this parameter Γ is in general small for high-viscosity fluids and large for low-viscosity fluids.

The calculated macroscopic contact angle θ_m is plotted in figure 7 (for an advancing liquid) as a function of $(Ca \ln \varepsilon^{-1})$ for various values of Γ for a typical example for which $\theta_w = 60^\circ$ and $\varepsilon = 10^{-6}$. It is observed that θ_m increases monotonically with increasing spreading velocity, reaching a value of 180° at a certain critical value of Ca (denoted by Ca_{max}) for all cases except when Γ is very small and we have the purely viscous situation where we have $\theta_m \to 180^\circ$ as $(Ca \ln \varepsilon^{-1}) \to \infty$. We also note, for fixed Ca, that $|\theta_m - \theta_w|$ increases as Γ decreases (i.e. for more-viscous liquids) if $\theta_m < 120^\circ$ but a more complicated behaviour exists for $\theta_m > 120^\circ$. The values of Ca_{max} for this example (with $\theta_w = 60^\circ$ and $\varepsilon = 10^{-6}$), from which the maximum spreading velocity may be determined, are plotted as a function of Γ in figure 8 (with $\theta_m = 180^\circ$).

It was assumed in obtaining the results shown in figures 7 and 8 for the above example that the microscopic angle had a value (60° for the example) which was

https://doi.org/10.1017/S0022112097008112 Published online by Cambridge University Press

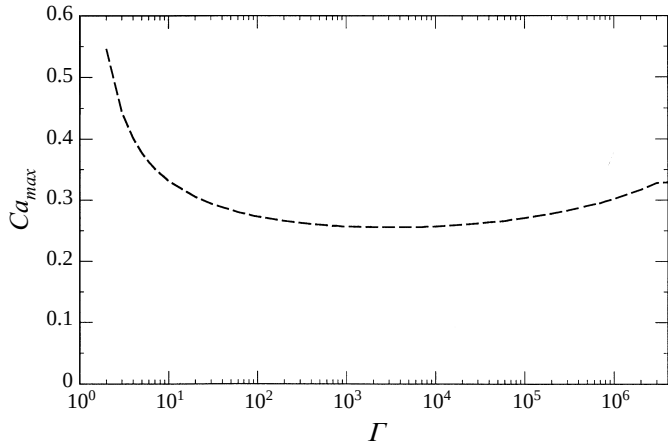


FIGURE 8. The maximum capillary number Ca_{max} for which a solution exists plotted as a function of Γ for an advancing contact line (corresponding to $\theta_m = 180°$).

constant independent of the spreading velocity U. There is, as pointed out by Cox (1986), some experimental evidence to suggest that for some systems at least, the microscopic contact angle θ_w is indeed a constant whose value depends only on the particular liquid and particular solid surface involved. The experimental results of Hoffman (1975) for silicone oils spreading on glass and of Hocking & Rivers (1982) for molten glass spreading on platinum (for which one had a viscous situation $Re \ll 1$) both agree with the hypothesis of θ_w being independent of the spreading velocity. However should there be systems for which the microscopic contact angle θ_w does depend on the spreading velocity, due perhaps to effects at the molecular scale, then the preceding theory and also the results listed in table 1 are still valid but with θ_w considered not as a constant but as a function of the spreading velocity. In fact the viscous and inertial effects on the liquid interface shape and on the macroscopic contact angle are always present and must always be considered (unless θ_w changes with spreading velocity U due to effects at the molecular level very much more rapidly than θ_m changes with U as predicted by the present analysis).

Since, due possibly to solid surface roughness or chemical heterogeneity (Johnson & Dettre 1964; Huh & Mason 1977*a*; Cox 1983; Jansons 1985), the contact angle in the static situation is, in general, not unique but can possess any value between the static receding contact angle and the static advancing contact angle, the question arises as to what value the microscopic contact angle θ_w should have if it is assumed constant (since in the present analysis all effects of solid surface roughness and chemical heterogeneity have been neglected). However the fact that in all our present results the macroscopic contact angle θ_m tends to the microscopic contact angle θ_w as the spreading velocity U tends to zero, suggests that θ_w should be taken as the advancing static contact angle for an advancing contact line.

This work was supported by the Natural Sciences and Engineering Research Council of Canada under grant A7007. Thanks are due to Ms L. Nardini for preparing the ms. in Latex form, to Dr P. Long for preparing figures 1–6 and to Dr J. Ferguson for undertaking the calculations that provided figures 7–9.

https://doi.org/10.1017/S0022112097008112 Published online by Cambridge University Press

REFERENCES

Burley, R. & Brady, P. R. 1973 *J. Colloid Interface Sci.* **42**, 131.
Burley, R. & Kennedy, B. S. 1976 *Chem. Engng Sci.* **31**, 901.
Cox, R. G. 1983 *J. Fluid Mech.* **131**, 1.
Cox, R. G. 1986 *J. Fluid Mech.* **168**, 169.
Dussan V., E. B. 1976 *J. Fluid Mech.* **77**, 665.
Dussan, V., E. B. 1979 *Ann. Rev. Fluid Mech.* **11**, 371.
Greenspan, H. P. 1978 *J. Fluid Mech.* **84**, 125.
Hocking, L. M. 1977 *J. Fluid Mech.* **79**, 209.
Hocking, L. M. & Rivers, A. D. 1982 *J. Fluid Mech.* **121**, 425.
Hoffman, R. L. 1975 *J. Colloid Interface Sci.* **50**, 228.
Huh, C. & Mason, S. G. 1977*a* *J. Colloid Interface Sci.* **60**, 11.
Huh, C. & Mason, S. G. 1977*b* *J. Colloid Interface Sci.* **81**, 401.
Invararity, G. 1969 *Brit. Polymer J.* **1**, 245.
Jansons, K. M. 1985 *J. Fluid Mech.* **154**, 1.
Johnson, J. F. & Dettre, R. H. 1964 *Adv. Chem.* **43**, 122.
Kennedy, B. S. & Burley, R. 1977 *J. Colloid Interface Sci.* **62**, 48.
Lowndes, J. 1980 *J. Fluid Mech.* **101**, 631.
Sakiadis, B. C. 1961 *AIChE. J.* **7**, 221.
Shikhmurzaev, Yu. D. 1997 *J. Fluid Mech.* **334**, 211.

https://doi.org/10.1017/S0022112097008112 Published online by Cambridge University Press